CHALMERS
UNIVERSITY OF TECHNOLOGY

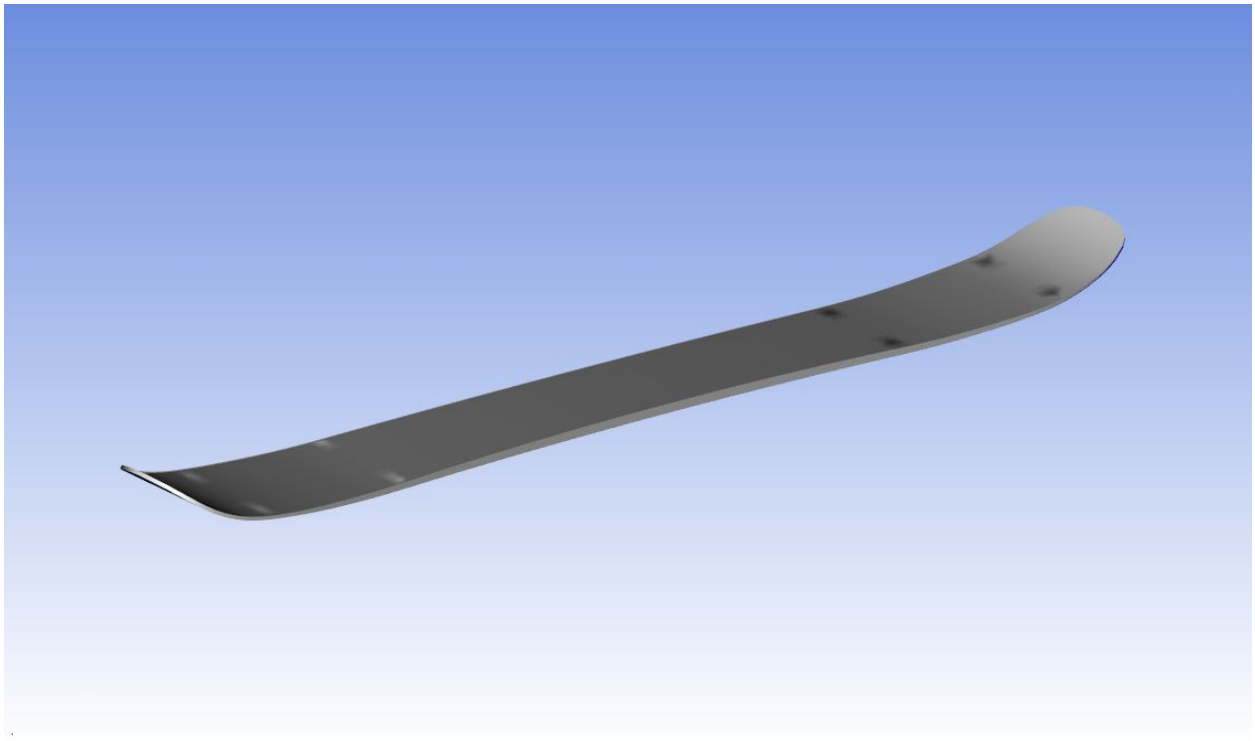

Ski development with Faction Skis: Product development and FE modelling of properties of alpine skis

Bachelor's thesis in Mechanical engineering

Department of Industrial and Materials Science
CHALMERS UNIVERSITY OF TECHNOLOGY
Gothenburg, Sweden 2018

Bachelor's thesis 2018:IMSX15-18-08

Ski development with Faction Skis: Product development and FE modelling of properties of alpine skis

John Borenius

Henrik Edman

Albin Lindmark

Marcus Pålsson

CHALMERS
UNIVERSITY OF TECHNOLOGY

Department of Industrial and Materials Science
Division of Material and Computational Mechanics
Chalmers University of Technology
Gothenburg, Sweden 2018

Ski development with Faction Skis: Product development and FE modelling of properties of alpine skis
JOHN BORENIUS
HENRIK EDMAN
ALBIN LINDMARK
MARCUS PÅLSSON

Supervisor: Martin Fagerström, Industrial and Materials Science, Chalmers University of Technology
Patrik Sannes, Faction Skis
Examiner: Brina Blinzler, Industrial and Materials Science, Chalmers University of Technology

Bachelor's Thesis IMSX15-18-08
Department of Industrial and Materials Science
Division of Material and Computational Mechanics
Chalmers University of Technology
SE-412 96 Gothenburg
Telephone +46 31 772 1000

Printed by Department of Industrial and Materials Science
Gothenburg, Sweden 2018

Abstract

When developing alpine skis, a lot of the work is based on previous knowledge and what has been done in the past. This report presents an approach to create an FE-model in conjunction with Faction Skis. The model is representing an existing alpine ski; the Faction Skis Candide 3.0, the model was developed with the intention of simulating the bending stiffness as well as damping coefficients and eigenfrequencies. After future improvement, the final goal of the model is to simulate new skis before prototypes are built, for a more fact based development process than in the past.

In order to obtain a reliable result, the model is compared to physical testing. A three point bending test and two different vibrations analyses were performed on a physical Candide 3.0 and compared to the FE-model. The collected data was then analyzed to determine the accuracy and predictive capabilities of the model.

A slightly deviant result of ca 7.2% is obtained when comparing the physical test results of the bending stiffness to the FE model's results. The deviant results are likely to have arisen due to non accurate material models as well as issues while establishing the thickness of each composite layer of the ski.

Two tests to determine the eigenfrequencies and the damping coefficients of the ski were conducted. Both found the fundamental eigenfrequency of the ski, but due to differences in the set up they differed somewhat, at 9 Hz and 9.75 Hz respectively. Damping coefficients were also found but varied more. Due to a lack of material damping data, damping was not implemented in the model but is a possibility for the future.
Even though the model does not fully correlate with the data from the physical test, it makes way for continued work. Future work is recommended to improve the accuracy and add damping capabilities to the model via more accurate material data. Adding breaking and shear strength prediction as well as delamination and progressive damage theory would also be interesting to enable the development of skis containing less conventional materials

Keywords: alpine skis, finite element modelling, bending stiffness, eigenfrequency, damping coefficient, Chalmers Sport & Technology. ANSYS Mechanical, ANSYS Composite PrepPost, three point bending, modal analysis.

Acknowledgements

This project was conducted at the Department of Industrial and Materials Science as a Bachelor's thesis in Mechanical Engineering.

There are several people involved in this project whom we would like to show our gratitude. First of all we would like to thank our supervisor Martin Fagerström, Associate Professor at the division of Material and Computational Mechanics, Department of Industrial and Materials Science, for supporting us throughout the project with guidance and knowledge. We would also like to thank Thomas Abrahamsson, professor in Structural Dynamics at the division of Dynamics, who helped us to set up the modal analysis and showed how to analyze the acquired data. Last but not least we would like to thank Patrik Sannes, former product designer at Faction Skis, and Sara Asmoarp, quality and sustainability manager at Faction Skis, for providing us with a deeper understanding of how the ski industry works.

John Borenius, Henrik Edman, Albin Lindmark and Marcus Pålsson,
Gothenburg May 2018

Contents

List of Figures

List of Tables

1

Introduction

Faction Skis, the industrial stakeholder of this project, is a small but ever growing ski company founded 12 years ago by a group of avid skiers. According to Faction Skis, their goal is to make products that push boundaries, rebel against the norm, last 100+ day seasons without servicing only to be thrown in storage for the summer and to be picked up the following year and be just as good as they were brand new. But more than anything, they aim to increase the fun factor of skiing, their skis have to be fun to ride. (Faction Skis, 2018).

The skiing industry is an industry in constant development, with new product lines every season. This creates an ambition and a need to find new creative ways to make skis that perform better, while being lighter and more durable. When developing skis new designs are often based on previously known facts and what has worked in the past according to Faction Skis' quality and sustainability manager Sara Asmoarp (personal communication, April 20th 2018). The current method of development based on experience makes it hard to predict the skis' mechanical properties, especially when using new materials.

This project intends to create and validate a finite element (FE) model of a ski. This is to better understand how it will behave under load and how different materials and composite layups will affect its mechanical properties before it's built. Using an FE model can also increase the speed and sustainability of the product development process, since it enables a faster, cheaper and more environmentally friendly way to get an idea of how a certain construction will perform. Faction Skis now former product designer Patrik Sannes acts as the industry liaison for this project. The fact that the project is researching FE modeling of composites also makes it interesting from an academic perspective since that particular area is an ever growing branch of engineering research and the theory in this project is applicable in many areas of the composite industry.

Physical studies of skis have been conducted by a team of Canadian researchers (Truong, Brousseau, & Desbiens, 2016). Although this study only looked at small linear deformations as opposed to the project at hand which looks to investigate larger deformations. The purpose of the Truong et al. (2016) study is to create a large database with stiffness values for as many already existing skis as possible, while the project at hand is aimed towards the development of skis.

Earlier composite analysis of skis have been conducted (Wolfsperger, Szabo, & Rhyner, 2016) although this analysis was made completely with solid models, directly in ANSYS' static structural toolbox as opposed to this project's shell model configuration along with ACP-toolbox. In this case a shell model was considered easier to parametrize and change for ease of use in the development process since ACP uses a single shell with composite layup data instead of several solid bodies and solid model data. The composite layup data from ACP can also easily be extracted into ply books to aid manufacturing personnel.

1.1 Limitations

The project only intends to establish means to test and simulate mechanical properties of skis, not to determine whether they are good or bad in terms of ski performance. The tests and simulations conducted in this project was limited to one ski, the Candide 3.0 which was provided in a 182 cm model from Faction Skis. In conjunction with Faction Skis, the bending stiffness along the ski's main axis, it's eigenfrequency and it's damping coefficient was chosen as the properties of interest.

The tip and tail of the ski in question consists mostly of Acrylonitrile butadiene styrene (ABS) plastic and does not affect the tests conducted in this project in a pertinent manner since the plastic parts are outside of the supports while testing, and was hence chosen not to be modeled accurately in the (FE) model.

The load cases chosen are not meant to represent the loads present while skiing, but are merely chosen for the ease of measuring, modeling and validating.

1.2 Outline

The report is divided into five sections, starting with the introduction which explains the purpose and background of this report. Following the introduction, the theory section is presented, aimed to give the reader all the theory and information needed to understand the rest of the report provided that the reader possesses basic mechanical knowledge.

The theory is followed by the methods section which explains the methods used during the creation and validation of the FE model.

The data acquired in the methods section is presented and analyzed in the results and discussion section. The section also discusses whether the results are along the lines of the research hypothesis presented in the introduction or not. Future research and improvement possibilities are also discussed.

In this final section the main conclusion is presented and the work is put in perspective to similar projects. The implications and consequences of the project is also discussed.

2

Theory

This section presents theory that has been applied in the project. The theory is intended to give the reader a better understanding of the methods and results presented in this report.

2.1 Structure of a ski

Most skis in the industry are made of a sandwich construction, as seen in Figure 1, containing layers of plastics, metal, fiber reinforcement, epoxy and a core according to Patrik Sannes (personal communication, February 6th 2018). The design of the lay up gives the ski different characteristics such as weight, stiffness, rebound, pop and durability in form of fatigue, long-term shear properties and impacts.

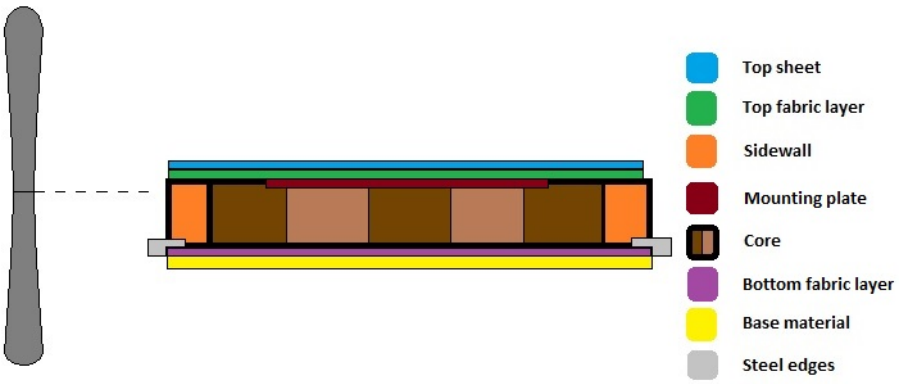

Figure 1: Graphic showing an example of a simplified sandwiched ski construction.

In the skiing industry the words rebound and pop are commonly used to describe the ski's spring like behaviour. For example the skier stores energy in the ski by flexing it while turning and when the energy is released it propels the skier out of the turn. The bending energy can also be used to achieve extra height when jumping. Rebound and pop are variables that are hard to quantify since the weight and strength of the skier plays heavily into how the ski is perceived. If the ski is to stiff a lighter skier will not be able to bend it and therefore will not be able to store energy in the ski and will hence not receive any pop from the ski. If the ski on the other hand is to soft a heavier skier will not be able to get any rebound out of it and hence a lot of the ski's important properties goes to waste (Patrik Sannes, personal communication February 6th 2018).

Faction Skis produces alpine skis in the freeskiing segment of the market. In turn, freeskiing is segmented into different areas such as touring, big-mountain, park and all-mountain skiing. Depending on the area, certain characteristics are favorable. A key mechanical property for every area is weight to solidity ratio which is affected by every layer in the ski.

Generally, the core of the ski is made from thin strips of wood glued together. It can also be made out of other materials such as foam. Depending on what material is chosen, the core receives different characteristics. Wood is a durable and responsive material, thus commonly used in the industry according to Patrik Sannes (personal communication, February 6 2018). Furthermore the wood fiber direction is of importance since different orientations give different mechanical properties and performance. It is preferable to have a core with many strips to reduce the risk of having weaknesses built in to the wood in form of knots, since knots do not have the same mechanical properties as the rest of the wood due to changes in structure and fiber orientation. Combinations of wood are often used to optimize the characteristics of the core. Low density wood, such as balsa for example, will result in a lightweight core, but may in turn be difficult to machine into thin ends due to wood chipping (Bcomp, 2018), while stiffer wood like ash are great sources of the aforementioned pop.

On most skis, layers of glass fiber reinforcement are placed both above and below the core to give the ski it's strength and durability. Some ski manufacturers chose to replace some of the glass fibre with carbon fiber to give the ski a higher stiffness. The fiber reinforcement can be set up in different directions to further change the mechanical characteristics of the ski. Layers of metal can be added for increased stiffness. These layers are normally placed above as well as below the core to prevent thermal bending caused by temperature changes. The base material is made out of a thin sheet of plastic made from extruded or sintered ultra-high molecular weight polyethylene (UHMWPE). These plastics are specially designed to absorb wax and to bond well with epoxy. The topsheet normally serves as a platform for graphics and is made of a thin plastic and therefore has minor impact on the characteristics of the ski according to Patrik Sannes (personal communication, February 6 2018).

Topsheets come in a wide variety of plastics ranging from polyethylene to P-Tex. A steel edge is integrated between the fiber layers and the base material to get grip on snow and ice. To protect the core from impacts and moisture damage, a sidewall made of plastic is placed along the edge. Also tip and tail spacers are inserted to reduce weight and make the core more manufacturable (Skibuilders, 2018).

2.2 Analytic solution of beam with laminate theory

The development of the the ski model was made step by step where the first step was to solve an analytic solution for a laminated simple beam for use as a reference before beginning to construct an FE model.

The following equations show an analytic method of solving a laminate beam bending problem, with a layup of several materials (Fagerström, 2018). The analytic solution was created to have a proven method to verify the initial FE model.

A coordinate system xyz is placed such that the x-axis points in the direction of the ski and the z-axis points out of the laminar plane. The displacement u in the x-direction that is located on the undeformed normal at a distance z from the midplane is given by

$$u = u_0 - z\alpha \tag{1}$$

where u_0 is the midplane displacement in the x-direction and α is the slope of the deformed section. If assumed that the normal plane is planar and perpendicular to the midplane also after the deformation, α can be found as

$$\alpha = \frac{\partial w_0}{\partial x} \tag{2}$$

where w_0 is the vertical displacement of the midplane in the z-direction. Combination of Equation (1) and (2) gives

$$u = u_0 + z(-\frac{\partial w_0}{\partial x}) \tag{3}$$

The in-plane strains can be derived as the strain component in the x-direction ϵ_x and the strain-displacement relation is calculated with

$$\epsilon_x = \epsilon_x^0 + zk_x \tag{4}$$

The midplain strains ϵ_x^0 and plate *curvature* k_x are defined as

$$\epsilon_x^0 = \frac{\partial u_0}{\partial x} \tag{5}$$

and

$$k_x = -\frac{\partial \alpha}{\partial x} = -\frac{\partial^2 w_0}{\partial x^2} \tag{6}$$

Using the equations above, the following equation for the x-direction is obtained

$$\epsilon_x = \frac{du}{dx} = \frac{du_0}{dx} + z(-\frac{d^2 w_0}{dx^2}) = \epsilon_x^0 + zk_x \tag{7}$$

Assuming uniaxial stress state, the stress in the x-direction is given by Hook's law as

$$\sigma_x = E_x \epsilon_x \tag{8}$$

where σ_x is the stress and E_x is the elastic modulus in the x-direction.

The stress resultant normal forces N_x and moment M_x are obtained by integration of stresses through the thickness of the laminate.

Resulting force per unit length in x-direction is given by

$$N_x = \int_{-\frac{h}{2}}^{\frac{h}{2}} \sigma_x \, dz \tag{9}$$

Resulting moment per unit length positive around the y-axis is given by

$$M_x = \int_{-\frac{h}{2}}^{\frac{h}{2}} \sigma_{xx} \, z dz \tag{10}$$

Combination of Equation (8) & (9) $\rightarrow$

$$N_x = \int_{-\frac{h}{2}}^{\frac{h}{2}} E_x(\epsilon_0 + zk)\, dz = \int_{-\frac{h}{2}}^{\frac{h}{2}} E_x\, dz\, \epsilon_0 + \int_{-\frac{h}{2}}^{\frac{h}{2}} E_x\, z\, dz\, k \tag{11}$$

Where $\int_{-\frac{h}{2}}^{\frac{h}{2}} E_x z\, dz = 0$ if layers are placed symmetrically around the central surface.

Combination of Equation (8) & (10) $\rightarrow$

$$M_x = \int_{-\frac{h}{2}}^{\frac{h}{2}} E_x(\epsilon_0 + zk)z\, dz\ = \int_{-\frac{h}{2}}^{\frac{h}{2}} E_x z\, dz\, \epsilon_0 + \int_{-\frac{h}{2}}^{\frac{h}{2}} E_x z^2\, dz\, k \tag{12}$$

A laminate consisting of n laminae, the normal force is obtained by:

$$N_x = \int_{-\frac{h}{2}}^{\frac{h}{2}} \sigma_x\, dz = \sum_{k=1}^{n} \int_{h_{k-1}}^{h_k} \sigma_x\, dz \tag{13}$$

where h_k and h_{k-1} is the z-coordinate of the upper and lower surface of lamina k respectively.

This gives the following result for Equation (12)

$$M_\alpha = \int_{-\frac{h}{2}}^{\frac{h}{2}} E_x z^2\, dzk = \frac{1}{3} \sum_{k=1}^{n} E_k(h_k^3 - h_{h-1}^3)k \tag{14}$$

Compare Equation (14) with classical Euler Bernoulli theory it is clear that $EI = \frac{1}{3}\sum_{k=1}^{n} E_k(h_k^3 - h_{h-1}^3)k$ can be seen as the equivalent bending stiffness of a beam with multiple layers. Thus, the deflection and cross section angle of a laminated beam can be calculated with an elementary case equation for simply supported beam (Sundström, 2016) with EI from Equation (14) as

$$\delta(a) = \frac{Fl^3}{3EI} a^2 b^2 \tag{15}$$

$$\theta = \frac{Fl^2}{6EI} ab(1 + a) \tag{16}$$

where δ is the deflection, F is the force, l the length of the beam, a and b is the proportion of length to where the force is applied and θ is the angle of deflection.

2.3 Finite element method

The Finite Element Method, abbreviated FEM, is a powerful method to approximate a continuous differential equation over an arbitrary geometry. The idea is to discretize the problem by dividing the geometry into a finite number of elements and by formulating the differential equation over these elements as numerical integrals. This results in a system of equations that can by solved effectively by computers (Ottosen & Petersson, 1992).

In general the method begins with a differential equation describing a balance between physical quantities, the so called strong form of the problem. During this project, the problem of linear elasticity is one equation that has been approximated using FEM. The balance equation for linear elasticity can be seen in Equation (17), where $\tilde{\nabla}$ is a differential operator, $\boldsymbol{\sigma}$ is a voigt vector of stress and $\mathbf{b}$ is a vector of body forces (such as gravity). According to Hook's generalized law, $\boldsymbol{\sigma}$ has to fulfill the constitutive relation seen in Equation (18), where $\mathbf{D}$ is the constitutive matrix which contains the elasticity of the material and $\boldsymbol{\epsilon}$ is the strain vector. The strain vector behaves according to Equation (19), where $\mathbf{u}$ is a vector of displacement

$$\tilde{\boldsymbol{\nabla}}^T \boldsymbol{\sigma} + \mathbf{b} = 0 \tag{17}$$

$$\boldsymbol{\sigma} = \boldsymbol{D}\boldsymbol{\epsilon} \tag{18}$$

$$\boldsymbol{\epsilon} = \tilde{\boldsymbol{\nabla}}\boldsymbol{u} \tag{19}$$

The equations above can be combined into Equation (20) which accompanied by boundary conditions, either as a vector of known displacement $\mathbf{g}$ or known traction (force per area) $\mathbf{h}$ as seen in Equation (21), gives us the strong form of the elasticity problem

$$\tilde{\boldsymbol{\nabla}}^T \boldsymbol{D} \tilde{\boldsymbol{\nabla}} \boldsymbol{u} + \boldsymbol{b} = 0 \tag{20}$$

$$\boldsymbol{t} = \boldsymbol{h} \qquad \boldsymbol{u} = \boldsymbol{g} \tag{21}$$

This form can rarely be solved directly, especially not for an arbitrary geometry. Finding an approximation for it is possible, but working with the differentials directly is not the most efficient or accurate way. Instead the differentials are rewritten on integral form into the so called weak form of the problem. For linear elasticity in three dimensions, this is done by first multiplying the strong form by an arbitrary test function $\mathbf{v}$, then integrating over the volume (Ottosen & Petersson, 1992) to obtain the weak form of the problem as Equation (22), with boundary conditions seen in Equation (21)

$$\int_V (\tilde{\boldsymbol{\nabla}}\boldsymbol{v})^T \boldsymbol{\sigma} dV = \int_S \boldsymbol{v}^T \boldsymbol{t} dS + \int_V \boldsymbol{v}^T \boldsymbol{b} dV \tag{22}$$

Unfortunately the integrals of the weak form can not be solved directly either. They have to be approximated numerically (the reader is referred to (Ottosen & Petersson, 1992) for more information on this) over regions that are easier to describe with mathematical functions than the general geometry. This is where the so called mesh comes in. It consists of a collection of geometrically simple bodies such as cubes and tetrahedrons which are arranged in such a way that they together approximate the general geometry. The behaviour of these shapes are governed by the same equations as the original problem, but they are easier to solve for. The solution to the original problem can, in a conceptual way, be described as the sum of the solutions to the many small problems, but put in relation to each other and their surroundings through the use of boundary conditions. For this project the software ANSYS was used to carry out the calculations and presentation of the results.

2.4 Modal analysis

To study the dynamical properties of mechanical systems, a modal analysis can be made. The goal is to identify the response of the system for a broad spectrum of frequencies when exited by an impulse, known as the frequency response. When the frequency response is known it is possible to predict how a system will respond to an impulse or signal. The response is important to know to be able to avoid effects such as resonance, which can cause unexpected behaviours and even the failure of systems (Schwarz & Richardson, 1999).

To conduct the analysis, the input signal (impulse) and output signal (vibration) are recorded. With known input and output signals, a transfer function relating them can be found. An assumption of the system behaving according to the reciprocity

principle, that the transfer function from a position 'A' to another position 'B' on an object is equal to the transfer function from 'B' to 'A', enables the system to be converted from a multiple input single output system (MISO) into a single input multiple output (SIMO) system. From this data, a model of the system can be established through system identification, the act of constructing a model of a system based only on statistics on the inputs and outputs without necessarily looking into what is physically happening inside the system .

After a successful system identification, a model of the frequency response of each of the locations which were originally subjected to an impulse will be known. From this model, information such as eigenfrequencies and damping coefficients can be found (Ljung, 1998).

2.5 Fast Fourier transform

The Fourier transform decomposes a function into it's frequency components and their amplitudes (James, 2011). A basic example of this is how a sine function in the time domain would become a single value representing it's frequency and amplitude after the transform to the frequency domain. From Fourier analysis it is known that any function can be represented as a sum of sine functions with different frequencies, amplitudes and phase shifts. This sum can be transformed to produce a new function in the frequency domain, representing the frequency spectrum of the original function (James, 2011).

A variation of the Fourier transform is the discrete Fourier transform which allows a discrete function to be analyzed in the same way as a continuous one. This enables a sampled signal to be analyzed, but the range of frequencies that can be found is limited by the number of samples and the rate of which they are collected. According to the Nyquist criterion, to be able to record a periodic signal, the sampling rate must be more than twice that of the frequency of the signal (Alciatore & Michael B. Histand, 2012). Otherwise aliasing will occur. Aliasing is when the original signal syncs with the sample rate to produce an artificial new signal. An example of this is when the shutter speed of a camera syncs with the rotational speed of a helicopter rotor, giving the impression of it being at rest when it's actually rotating fast. It is also important that the sampling has low jitter (Intergrated, 2018), that they are collected at a constant rate. Otherwise the samples will represent the wrong frequencies and produce a lower signal to noise ratio. A problem with the discrete Fourier transform is that it's very computationally heavy.

The fast Fourier transform (FFT) is an algorithm that dramatically increases the speed of which the discrete transform is calculated. It utilizes that sample numbers chosen as powers of two reduces the number of multiplications needed to compute

the transform and thus the computational time as well (James, 2011).

2.6 Vibration theory

The amplitude of an under damped system decreases in a logarithmic fashion. For such a system, the damping ratio can be derived from data of the system's motion using the amplitude of two consecutive peaks of the motion. This relation is called the logaritmic decrement method and is defined by the following formulas, where ζ is the damping coefficient, *x(t)* is the amplitude of a peak, n is the number of periods between two peaks and T is the period of the motion.

$$\delta = \frac{1}{n} ln \frac{x(t)}{x(t+nT)} \tag{23}$$

$$\zeta = \frac{1}{\sqrt{1 + (\frac{2\pi}{\delta})^2}} \tag{24}$$

The frequencies of damped; ω_d and undamped; ω_n systems are not equal, but they correlate according to the relation below. If the damping ratio approaches zero, the damped frequency approaches the undamped frequency.

$$\omega_n = \frac{\omega_d}{\sqrt{1 - \zeta^2}} \tag{25}$$

If an under damped system is of order one, that the motion has only one mode, and its frequency and damping coefficient is known. Then the motion of the system can be described using the following mathematical model. Where A is the initial amplitude of the motion, e is the natural logarithm and ω is the angular frequency (Grahn & Jansson, 2013).

$$x(t) = Ae^{-\zeta\omega t} sin(\omega t) \tag{26}$$

3

Methods

To understand the behaviour of the ski a deeper knowledge about design and components is required. This is also important in order to make a valid FE model. The method section describes the steps from collecting data for the initial analytic solution on a composite beam to the final model.

3.1 Material data

Data was gathered to provide information about the mechanical properties of materials often used in skis. The choice of materials to research was based on what Faction Skis have used in the past. Faction Skis has gathered experience on how different materials performs and feels while skiing, which is of importance since a theoretically advanced ski with optimized characteristics may not be equivalent to a ski that is enjoyable going down a slope. This is however information that can not be disclosed in this report. To get a hold of material data, the main sources of information was from Faction Skis, their suppliers and the material database Cambridge Engineering Selector (CES), (Granta Material Intelligence, 2018). Some of the information about wood types was also collected from a website called the wood database (Meier, 2018). For this project, The Orthotropic Youngs' moduli, Poisson's ratio were important mechanical properties to gather, needed for the bending stiffness calculations. The most common materials used are poplar, beech, ash, balsa, paulownia, flax, glass fiber, carbon fiber, ABS, Titanal, steel and epoxy according to P. Sannes (personal communication, February 6 2018). The material properties were found in CES and have variances in hardness, density and compressive strength (Granta Material Intelligence, 2018). Data of the common materials was found via the mentioned sources and placed in an Excel-file to serve as a material database for easy access and overview. The material database can be found in Appendix H, although it is revised due to disclosure agreements with Faction Skis. AMAG

Titanal®, mentioned above, is a high strength, age hardenable aluminum-wrought-alloy. The material characteristics such as formability and bonding capacity makes it usable as a supporting element in composite skis. Bonding in composites, e.g. with epoxy resin adhesives is achieved with a thin, open pore phosphoric acid anodized layer. The material provides torsion-resistance, smooth running, edge grip and vibration damping. (AMAG, 2018).

3.2 Analytic solution of composite beam

To verify that the results of the initial FE model was reasonable, an analytic solution was made for reference use. A layup, see Table (1), of three different materials with known Youngs' moduli used in the Candide 3.0 ski were chosen for the analysis. The amount of material per layer was chosen to work with Equation (13) since it can be applied if symmetry around central surface prevails. Therefore the same amount of material was placed around the central poplar laminate. The different stiffness and positions of the layers were converted into an average using Steiner's theorem. By doing this, classic Euler-Bernoulli beam theory could be used to calculate deflection.

The analytic stiffness solution, was calculated with Equation (13) and values from Table (2) to get the EI value for the laminate. Youngs' moduli data was collected from the material sources and dimensions were based on the lay up in Table (1) and the width was chosen to be similar to the actual central width of the Candide 3.0 ski.

Glass fiber [2 mm]
Titanal [0.6 mm]
Poplar [10 mm]
Titanal [0.6 mm]
Glass fiber [2 mm]

Table 1: Table showing the layup used for the analytic solution of a composite beam.

$E_{titanal} = 75$ GPa
$E_{glassfiber} = 20$ GPa
$E_{poplar} = 10.9$ GPa
$height = [0, 2, 2.6, 12.6, 13.2, 15.2]$ mm
$w = 0.1$ m

Table 2: Table containing material data for the composite beam.

The EI value was calculated per unit width and therefore had to be multiplied with the width of the lay up to get the total value, $EI_{tot} = EI * w$. Further calculations on the deflection was made using Equation (15) and following data on force and length: $F = 600$ N, $l = 1$ m, $a = 0.5$ m, $b = 0.5$ m. The data was implemented and calculated in MATLAB, see Appendix A.

3.3 Creating the ski model

The finite element model made for the Candide 3.0 ski was performed with the finite element software ANSYS Workbench 18. Early in the project it stood clear that to produce a good model in the time available, the ability of the chosen FE program would have to be very good at modelling composites, be as user friendly as possible and have good resources for support. ANSYS provides all of this as well as opportunities to recieve live support from ANSYS personnel were arranged by the Mechanical Engineering program at Chalmers. All of this in combination with some basic personal experience resulted in the decision to use ANSYS Workbench 18.

The following sections describes the development from simple beam calculations to the final FE model with the correct geometry and lay up for the Candide 3.0. It was essential to carry out the progress through simple well defined steps. By doing so, it was easy to evaluate what was working and what was not. In the case of a more advanced model failing, places to fall back to were available.

3.3.1 Simple composite beam

A model of a simply supported composite beam with a rectangular cross section was created to verify that ANSYS' ACP-toolbox was in line with the analytical solution in Section 3.2. ACP-toolbox was used because of its powerful tools for analyzing and designing layered composites. It is effective for defining fiber orientation, layup modification, model inspection, and parameterization of material properties which is of importance to this project (ANSYS Inc., 2018).

The lay up chosen, was the same as presented in Table 1. The material properties for the materials shown in Table 2 was taken from the material database mentioned in Section 3.1 and inserted to engineering data in ANSYS. The same force was applied on the beam as in the analytic solution and the FE-analysis deflection of the beam matched the analytical solution to a tenth of a millimeter. The beam is shown in Figure 2.

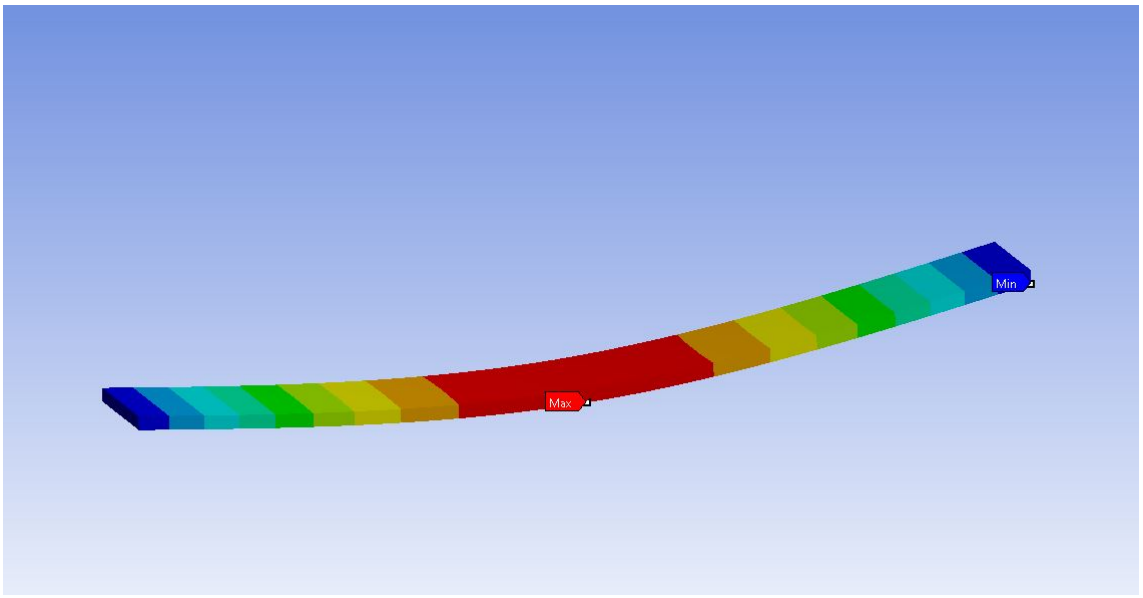

Figure 2: Render of the simple composite beam modelled in ANSYS.

3.3.2 Implementation of a variable thickness core and correct geometry

Following the simple beam, a simple ski geometry was created in the computer aided design (CAD) software Autodesk Inventor (Autodesk Inc., 2018) to verify that CAD geometries could easily be imported to the ACP toolbox. The successfully imported geometry can be seen in Figure 3. The initial ski model had a square cross section and no camber so that it would still be considered a simple beam and thus could easily be compared to the analytic studies. The results from this model was in line with the analytic solution and the work was continued.

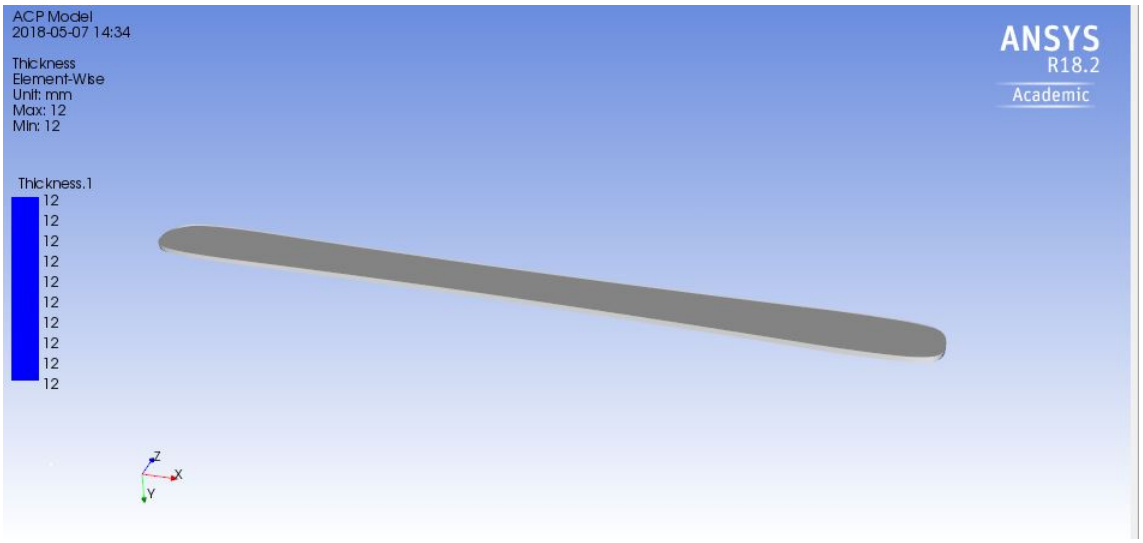

Figure 3: Render of a simple ski model in one plane with a core of constant thickness.

The next step to improve of the model was to gather data from drawings and construction sheets for the Candide 3.0 supplied by Faction Skis. The construction sheet contained information on the lay up; materials used, what amount and type of fiber composites as well as fibre directions. The drawings and construction sheets contained the dimensions needed to make a model of the ski, including core thickness variations.

The information was first used to create a model with the correct geometry of the ski, while still retaining the square cross section for easier comparison with the earlier FE and analytical models. As the core of a ski varies along it's span, thinning out towards the ends, and one of the validation methods was a wide span three point bending test, the next logical step was to create a model with a variable thickness core. This was achieved with tabular data with thickness measurements along the length of the core received from Faction Skis along with a built in function for tabular reading in ANSYS' ACP-toolbox. Since the core of the ski is made up of wood strips with different stiffness, an average of the different materials' stiffness was implemented to the core in ANSYS. This model is seen in Figure 4.

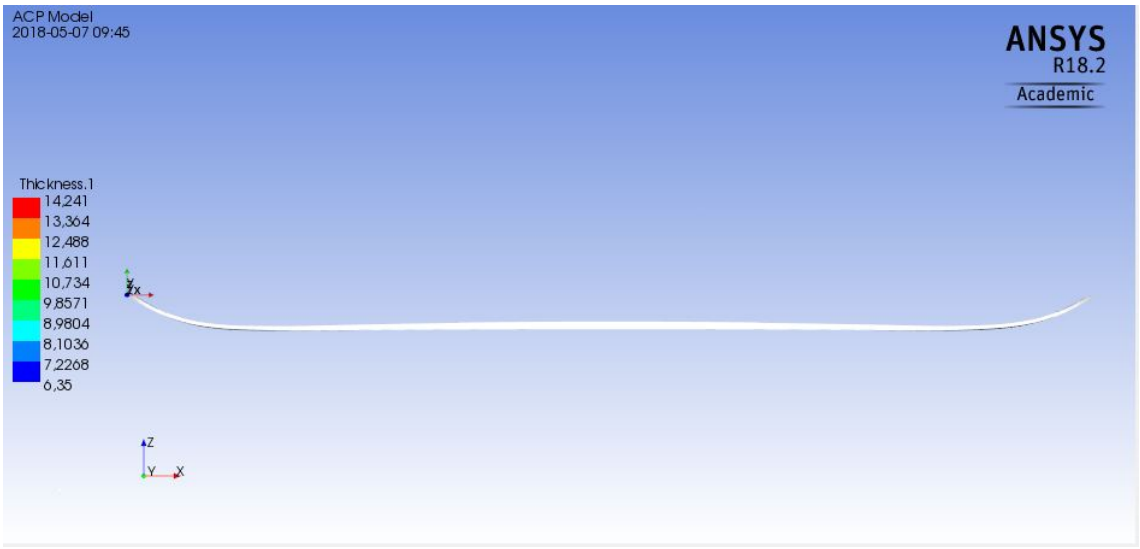

Figure 4: Render of the ski with a variable thickness core and correct geometry.

3.3.3 Final model

The final step of the model was to implement all construction elements given by the construction sheet supplied from Faction Skis. In table 3 the layup of the ski and final model can be seen. This model would later be the basis for future construction changes. A more detailed layup can not be presented due to disclosure agreements with Faction Skis.

Top sheet
Sidewall
Top fabric layer
Mounting plate
Core
Bottom fabric layer
Base material
Steel edge

Table 3: Table showing the layup for the Candide 3.0. For the final model the topsheet was excluded.

The previous average Youngs' moduli for the core were changed to a core with strip glued wood seen in Figure 5. The size of the strips was determined by measuring a wood core from a disassembled Candide 3.0 ski, provided by Faction Skis, see Figure 6. The method used was to divide the core in the existing Inventor model of the ski into strips. When imported to ANSYS, the strips can be appointed a named selection which is then transferred to Oriented Selection Sets in ACP where the correct materials are then applied.

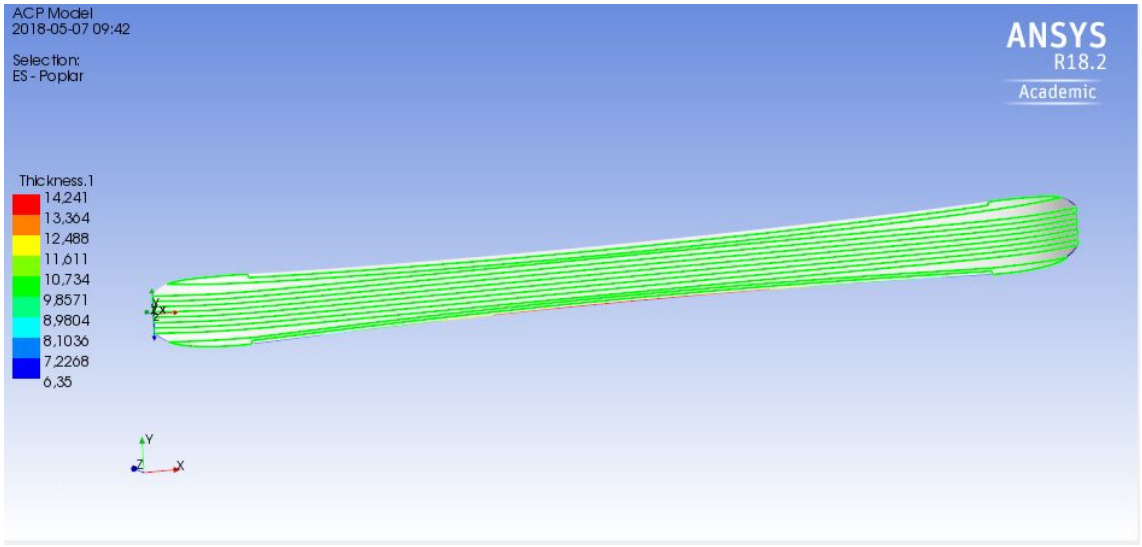

Figure 5: Graphic of FE model with core strip distribution showing.

Figure 6: Picture showing a section cut of the Candide 3.0.

The design of the steel edge was based on a drawing from (Waelzholz, 2014). The steel edge and sidewall was modeled in Inventor, (see Figure 7) and analyzed in ANSYS Static structural to acquire stress/strain values from which the equivalent Young's modulus could be calculated with Equation (27) via five average stress and strain measurements. A strip with the aforementioned equivalent Young's modulus was inserted along the edges of the core.

$$E_{eq} = \sum_{i=1}^{n=5} \frac{(stress_i/strain_i)}{n} = 27.192GPa \tag{27}$$

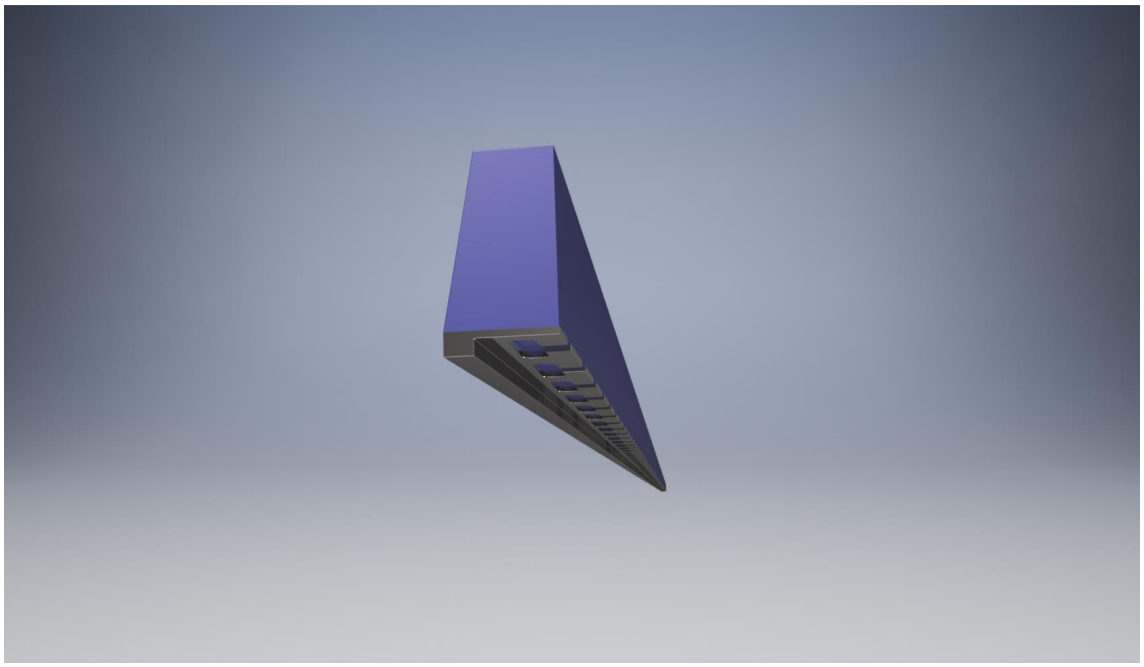

Figure 7: Render showing the edge - sidewall combination used to calculate the edge equivalent stiffness.

Furthermore, the top and bottom fabric layers were inserted into the model. The construction sheet was used to apply the right amount of glass fibers in certain directions, implemented in ANSYS' ACP-toolbox. The tip/tail spacers effect on three point bending test was estimated to not affect the results since they are not placed between the supports where the bending occurs, see Figure 8. Therefore they were excluded from the data model and the core filled their place.

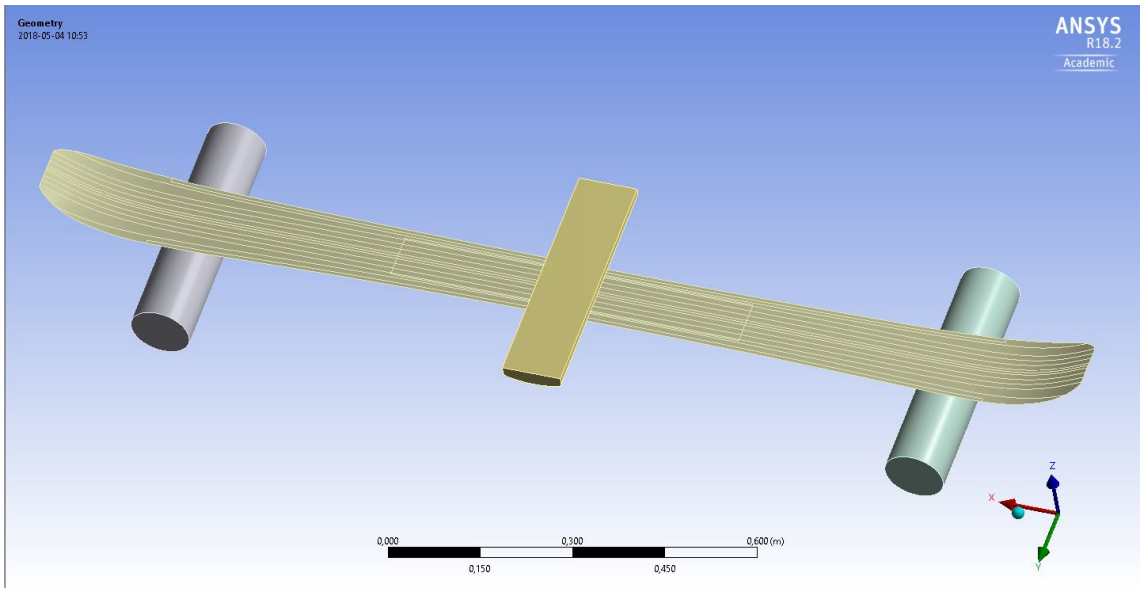

Figure 8: Graphic showing the virtual three point bending test.

Since the core is partly made of balsa which is a soft wood, a mounting plate of Titanal exists for a secure mounting point for the binding screws. The base material is made of plastic and inserted in the model as a laminate in ANSYS. The top sheet made of thin plastic, majorly acting as a surface for graphics and was considered not to greatly affect the result of the final model in a bending test and due to a time limit it was excluded from the data model. A render of the complete ski can be seen in Figure 9.

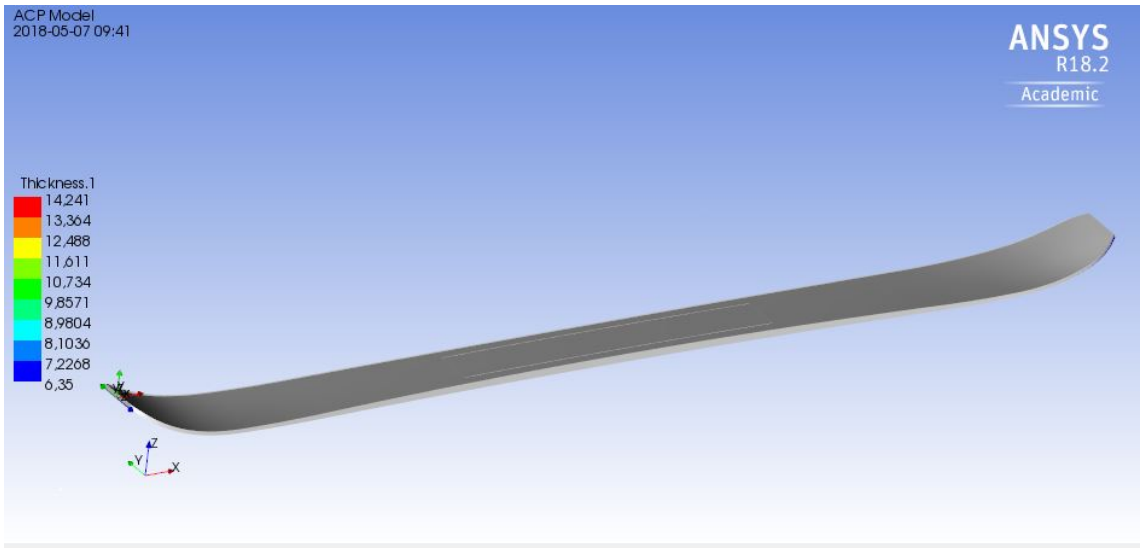

Figure 9: Render showing the final model in ANSYS.

Finally the method of computation was changed from linear to non linear to better suit the large deformations of the three point bending test. A simulated deformation is shown in Figure 10.

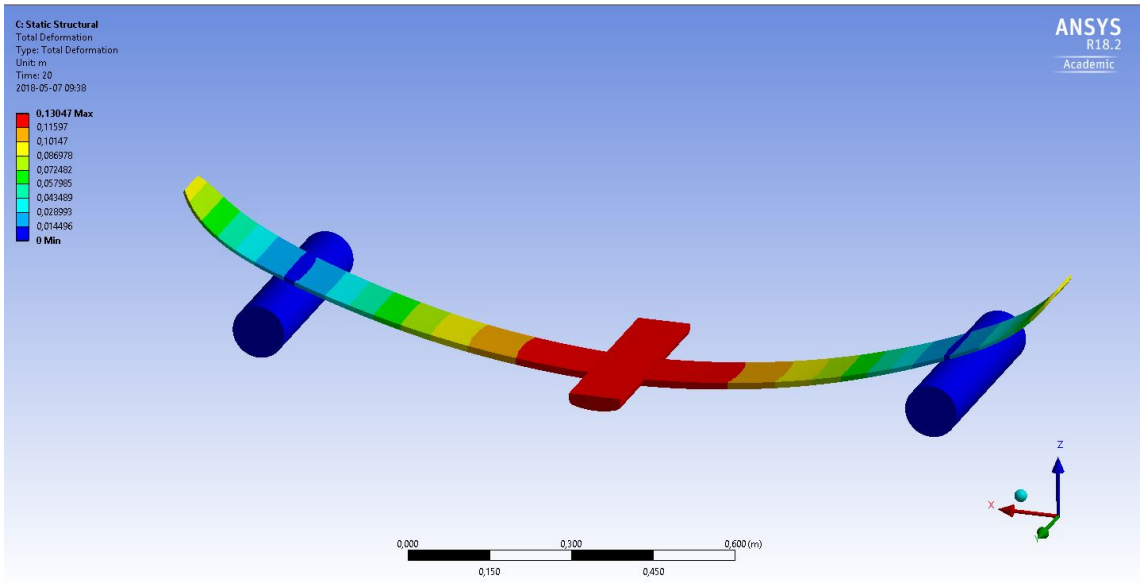

Figure 10: Render showing the deformation of the final model in ANSYS.

3.3.4 Sources of error for the final model

Only a few select mechanical properties of the composite materials used in Factions skis are available to the project, which in itself presents a source of error. The material suppliers specified a certain stiffness which seemed quite low for standard glass fibre reinforcement. Patrik Sannes at Faction Skis deemed theese values low, while discussing materials at a meeting, February 6th 2018 and made an assumption of the stiffness based on experience which was higher than the manufacturer's. Results based on both the manufacturer's and Sannes' values are presented in Section 4. The particular values can be found in Appendix H, although the data is revised due to disclosure agreements with Faction Skis.

Since the steel edge and polymer sidewall were modeled together and the equivalent Young's modulus was estimated through simple calculations (see Subsection 3.3.3) an apparent source of error can be found here.

The thickness of each layer in a ski is difficult to estimate since the ski is press molded with a pressure of ca. 0.7-0.9 MPa according to Faction Skis representative Patrik Sannes (personal communication February 6th 2018). The thicknesses chosen for the model was based on the thicknesses the material suppliers used when conducting tests to acquire material stiffnesses. The total thickness of the model was found to be ca 1 mm (7.7 %) thicker than the actual ski which presents a definite source of error. The excluded top sheet from the laminar lay up is a source of error since it will provide some stiffness.

3.4 Test rig

To validate the FE model of the ski, a physical test was constructed. This test had to be suitable for evaluating the mechanical property in question; bending stiffness, and be easy to conduct both virtually and in reality. For these reasons, the three point bending test was chosen. It is simply the structure in question supported between two support rollers and subjected to a normal force from a tool at the center of the ski. The deflection in relation to the force applied is used to determine the stiffness of the structure.

The mechanical engineering department at Chalmers Institute of Technology provided a uniaxial compression test machine that is able to apply force and measure the deflection. To accompany the machine, two supports and a tool to apply load had to be simulated and manufactured. The tool and supports are described in Subsections 3.4.1 and 3.4.2, and simplified drawings are found in Appendix G.

3.4.1 Supports

The design of the supports, see Figure 11 and 12, was governed by three demands. A basic first demand is for the supports to remain stable and safe during the whole load cycle. The ski is elastic and a lot of energy is stored in it when it is under load. By the nature of the test, the angle of the contact force between the ski and the support change during loading which could cause a support to tip over. Therefore the legs of the supports were designed so that the moment caused by the normal force of the ski would always push the supports securely into the ground and never reach a tipping point. It was decided that no test with a deflection larger than 15 cm would be made. Using this value and the stiffness derived in Section 2.2 and Equation 16, a maximum angle of the ski at the contact point to the supports was estimated to be 19.8°. The angle of the legs was therefore chosen to 30°, assuring stability. Two horizontal square tubes were also fitted to keep the supports from sliding apart.

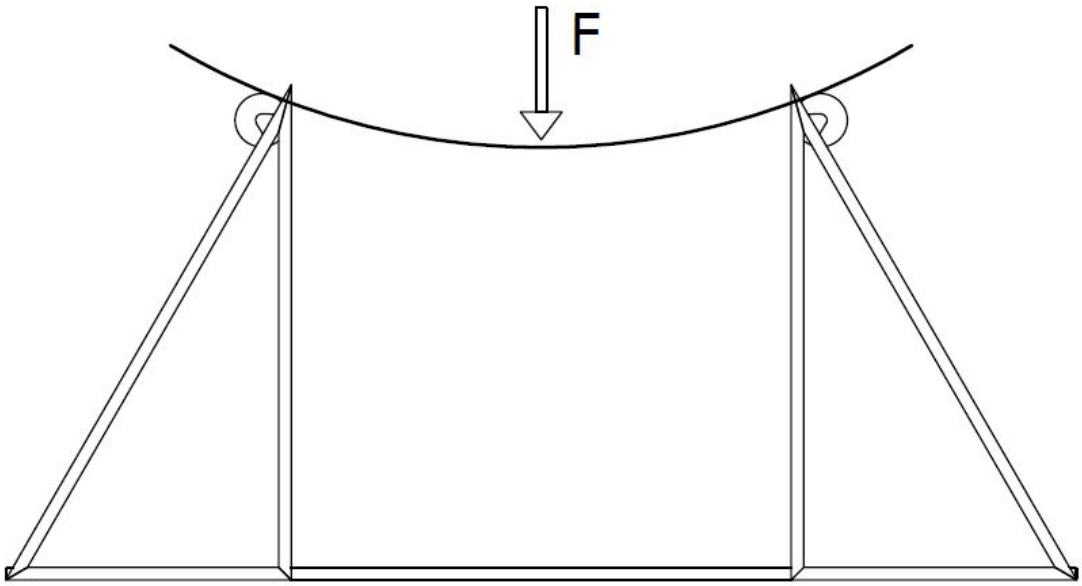

Figure 11: Simple sketch showing the layout of the test rig supports.

A second demand was for the rig to simply support the ski while still being simple to model in ANSYS. In the FE model described later in this section, the ski is supported on two frictionless rollers which means that the ski is allowed to move freely in the direction along the ski while still being held in the vertical plane. To be as close to the model as possible, the supports were designed with bearing-supported rollers for the ski to rest on. The ski was modeled to only travel in the vertical plane at the ski center since a lot of friction between the displacement tool and the ski held the ski in place in the test rig.

The third demand was for the supports to have very little deformation in relation to the ski, to not obscure the data. For this reason an FE model was made and can be found later in this section. The result of the analysis was that square tubes of the dimensions 30x30x2 mm would give sufficient support and very little deformation. These tubes were welded together, apart from the two horizontal bars which were bolted to the rig to enable storing. The height of the test rig was chosen to fit the uniaxial compression test machine. The width between the rollers was chosen to be 1300 mm to exclude the ski's softer ABS tip and tail.

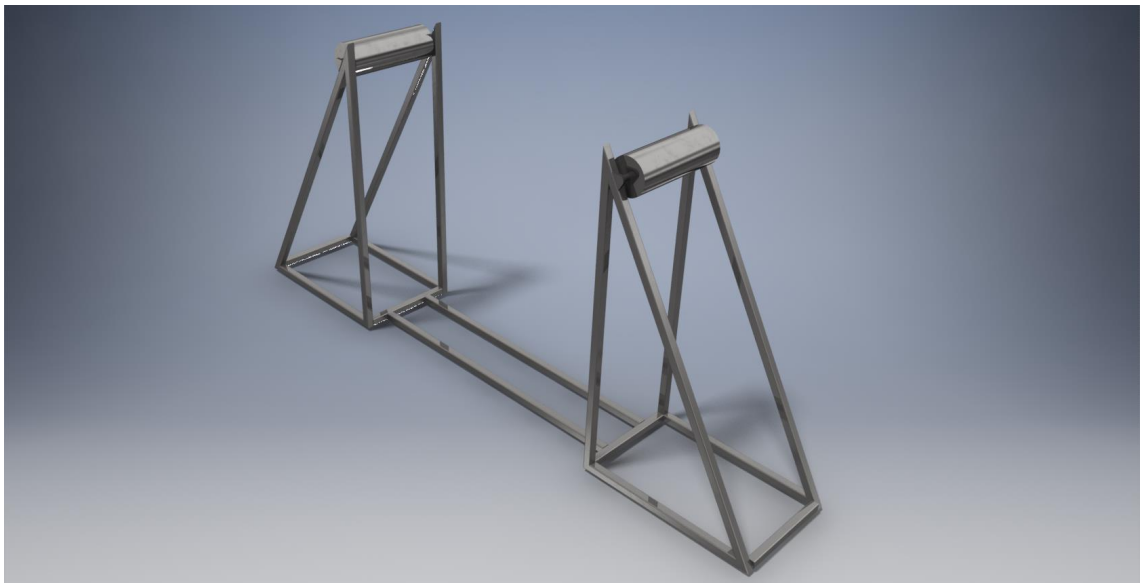

Figure 12: Render of the test rig used for the three point bending test.

Since the deformation of the rig was a possible source of error, an FE model of the frame and the rollers was created to analyze their deformations, see Figure 13 and 14. The maximum total deformation of the rig was shown to be less than 1 mm, the rig's deformation was therefore disregarded. Worth to mention is that the dimensions of the analyzed test rig does not completely match the actual rig but it still has the same shape. In the analysis of the test rig supports the built-in frame generator and frame analysis in Autodesk Inventor was used since it is considerably faster than ANSYS because a lot of the functions in ANSYS would not be needed. The analyzed frame was constructed of 30x30x2 mm steel square tubing, although 30x30x1.5 mm tubing was used for the actual construction in cooperation with the engineers at Chalmers Prototype Laboratory, with the reasoning that the deformation of the 2 mm model was only 0.05 mm, the change to 1.5 mm would not give a deformation significan enogh to affect the actual testing of the ski. There were also minor changes made to the dimensions in the physical test rig but these changes were considered not to have a pertinent effect on the test rig.

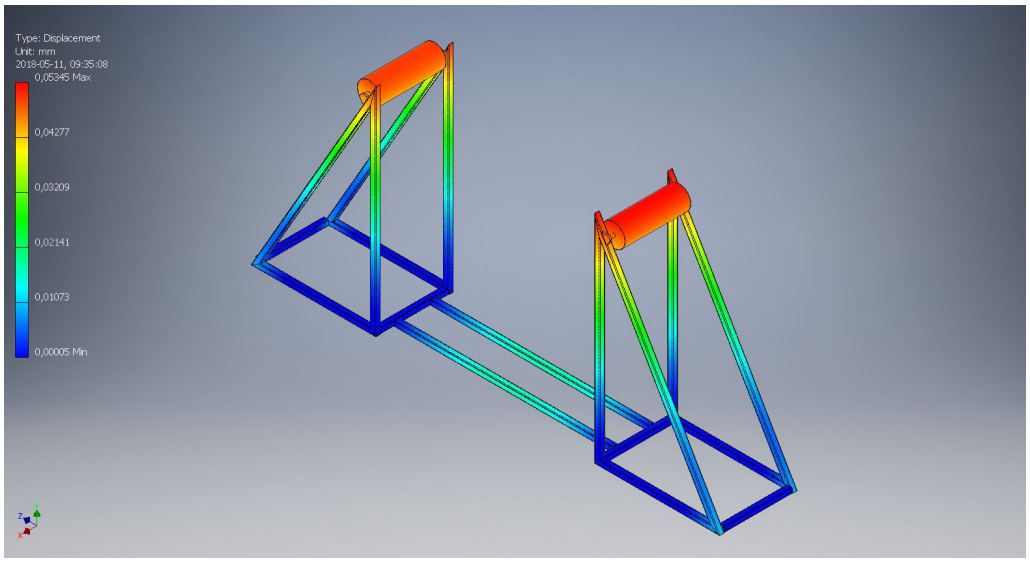

Figure 13: Render showing the deflection of the supports under the loading of a three point bending test.

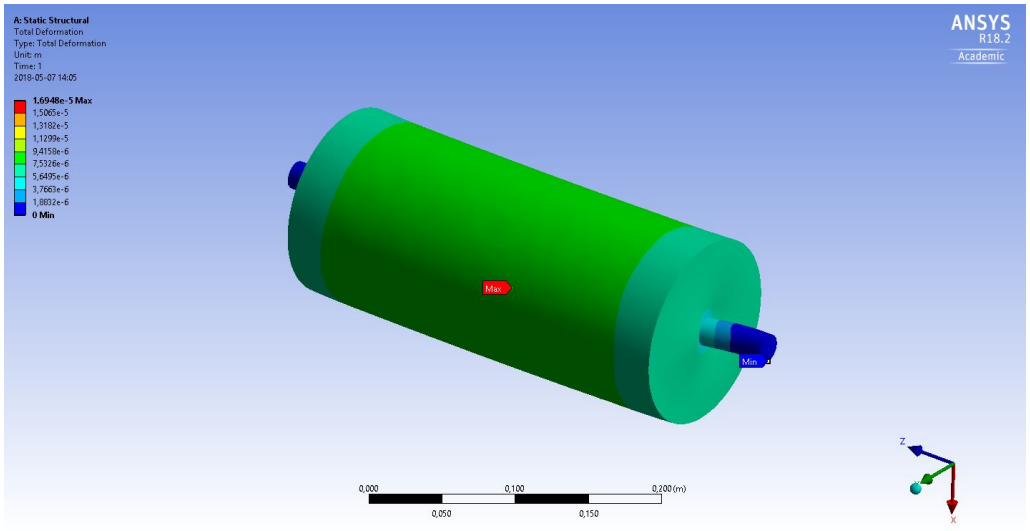

Figure 14: Render showing the deflection of a support roller under the loading of a three point bending test.

3.4.2 Tool

In order to apply force to the ski with the uniaxial compression test machine, a tool was engineered and manufactured. Concerns surrounding the ability of the composite to handle the pressure from the tool arose. Two designs were created with the aim to distribute the load over a larger area. One of the designs was a rounded surface with a radius that was as large as possible while still smaller than the radius of the bent ski, not to influence the bending of the ski, so that the

force would be more spread out. The other design was a square block with rounded corners. The latter design would distribute the pressure over two smaller areas when the ski is bent which is undesirable for this application since it would no longer be a three point bending test. Thus, the single radius tool was chosen and tested for contact pressure which is addressed in the paragraph below.

A concern before conducting the bending test was that the contact forces between the tool and the ski during the test would surpass the compressive strength in the normal direction of the ski. Thus, an analysis of the contact forces between the tool, the ski and the supports was made. A render of the calculated contact forces, which are well bellow the aforementioned compression strength, can be seen in Figure 15. The simulated pressure of 2.2 MPa was well bellow the compressive strength of 57.8 MPa for pure epoxy which is lower than that for glass fibre reinforced epoxy (Loos, Coelho, Pezzin, & Amico, 2008).

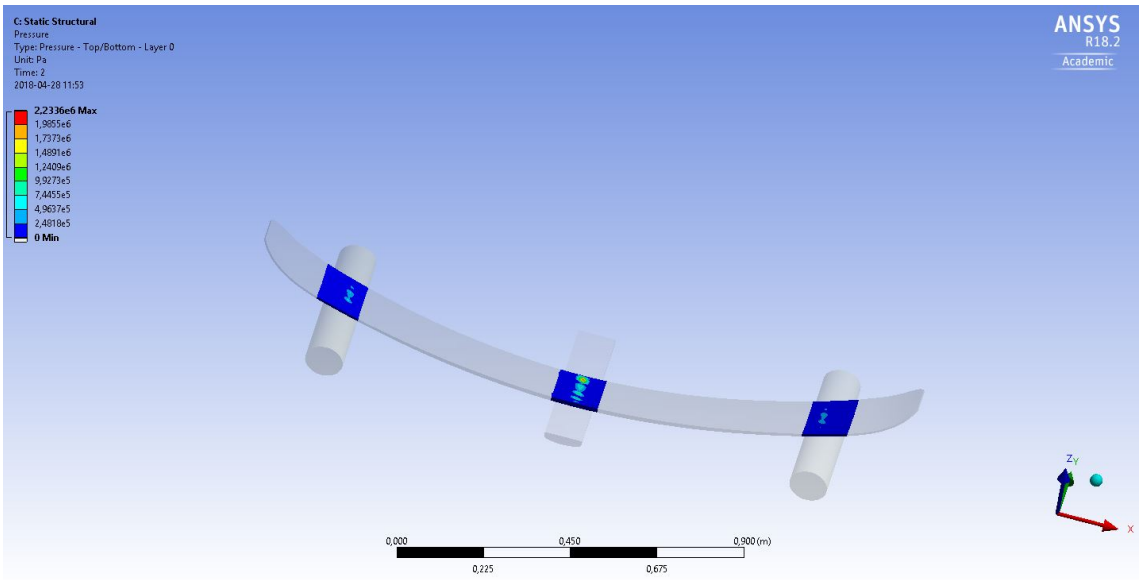

Figure 15: Render of contact pressures between tool, ski and rollers when load is applied via the tool.

The CAD-drawing (see Appendix G.2) of the tool was exported to a CAM-software and manufactured with a CNC-mill at the prototype laboratory at Chalmers, see Figure 16. The finished tool can be seen in Figure 17 and Figure 18. The tool mounted to the machine can be seen in Figure 19

Figure 16: Picture showing the tool mounted in the mill after the first operation.

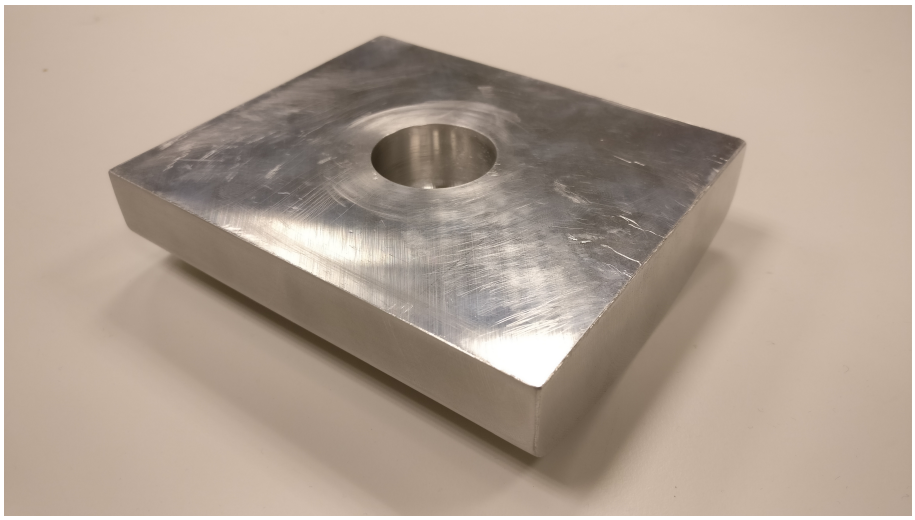

Figure 17: Tool for applying force onto ski, hole for connection to uniaxial compression test machine via slight press fit visible.

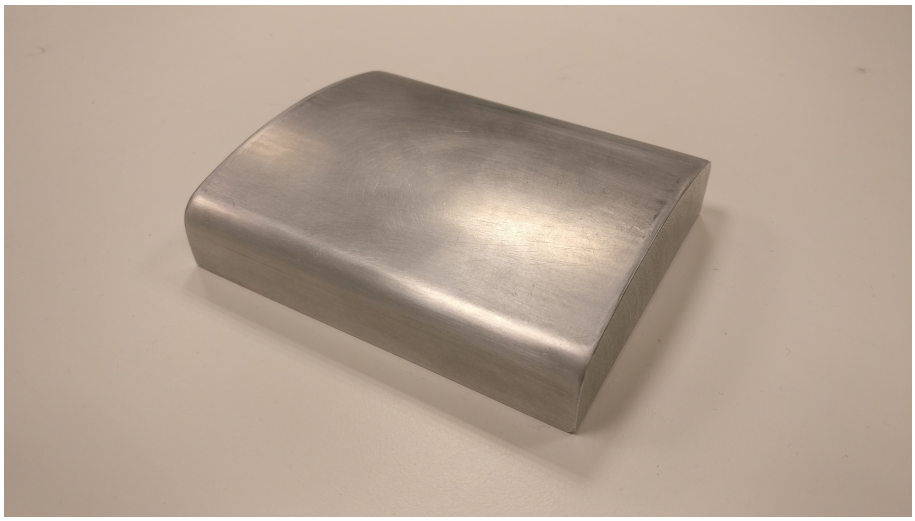

Figure 18: Tool for applying force onto ski, rounded smooth side for contact with ski visible.

Figure 19: Picture of tool mounted via press fit in the uniaxial compression test machine

3.5 Physical testing

This section describes the process of the physical testing made to validate the FE model. The ski was placed on the test rig with the tool placed in the middle as shown in Figure 20.

Figure 20: Picture showing the three point bending test on Candide 3.0.

The uniaxial compression test machine displaced the center of the ski 130 mm while simultaneously collecting data about load and deformation. The test was repeated eight times for the Candide 3.0 ski to detect deviations in the collected data. The ski was also moved and rotated 180° in between the tests to see if the results are reliable. The deformation-force data from the eight different tests was retrieved and in order to compare the different results the data had to be reformatted as described in Section 3.6.

3.6 Comparing bending test results

The collected data from the simulated and physical three point bending test was imported to MATLAB where it was mathematically compared. The data was collected at different points between 0-130 mm. To obtain a comparable result the deformation-force data had to be represented at the exact same points and was therefore interpolated. All of the deformation data was interpolated at 500 points between 0.01-130 mm. A mean value of the physical testings' applied forces was obtained for the interpolated points and then compared to the results from the ANSYS simulations, the results of which can be seen in Section 4.

The deviation for the ANSYS model's applied force from the physical test is calculated for each point of deformation. A total mean is then calculated of the sum of the force deviations to be able to analyze the result as a whole. The code used to perform the comparison is presented in Appendix B.

3.7 Vibration analysis

According to Faction Skis, the dynamical properties of skis are just as important as the static properties. Every skier know that the behaviour is completely different from ski to ski and is key to their performance, but it can be very hard to effectively and objectively quantify these differences. Therefore it would be valuable to establish a test to take measures from. Two important properties that determine the dynamical behaviour of a system is the eigenfrequency and the damp coefficient. Two efforts to measure these properties for skis have been made. One simple vibration test was developed that can be made quickly and cheaply. Another test made with laboratory equipment provided by Chalmers was also conducted.

3.7.1 Simple vibration analysis

If the tip is subject to an impulse while skiing, for example a disturbance in the snow, the composite of the ski behaves as an under damped cantilever beam in front of the binding. This means that the motion following the impulse has several oscillations before it comes to rest. Given the size and weight of the ski, oscillations has a relatively long period and large amplitude at the tip. This motion can easily be observed with the naked eye and it was theorized that it was possible to measure this oscillation with very simple sensors. The damping coefficient and the eigenfrequency of the ski can then be derived using the logarithmic decrement method and the fast Fourier transform, see Section 2.6 and 2.5. These two parameters describe much

of the dynamic behaviour of the ski and it is valuable to easily be able to measure these.

3.7.1.1 Design

The test was designed as described in this paragraph. The ski was mounted securely to a very stiff and dense structure at boot center and backwards. In this case, a welding table with several clamps was used. Above the ski's front end, a sensor was mounted to a pole placed next to the ski on the concrete floor. The sensor then measured the movement of the ski following an impulse. The ultrasound distance sensor HC-SR04 was chosen along with an Arduino Uno for the data logging, see Figure 21 and Figure 22. The Arduino sends out a pulse width modulation (PWM) signal to the sensor which creates an ultra sound pulse. The sensor then measures the time for the pulse to reflect back. This data was logged by the Arduino and sent using the universal serial bus (USB) to MATLAB were analysis took place using its built in function called fft (Mathworks Inc., 2018). The complete physical set up can be seen in Figure 23, the code can be found in Appendix F.

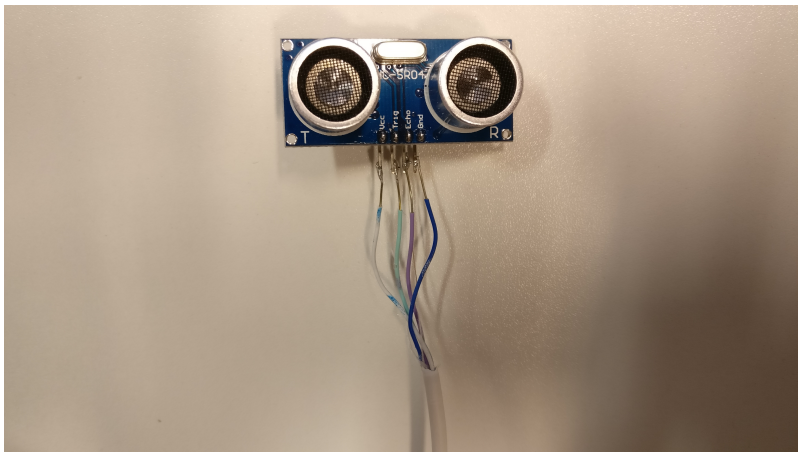

Figure 21: Picture showing the HC-SR04 sensor that was used to measure displacement over time of the ski when it was set into motion.

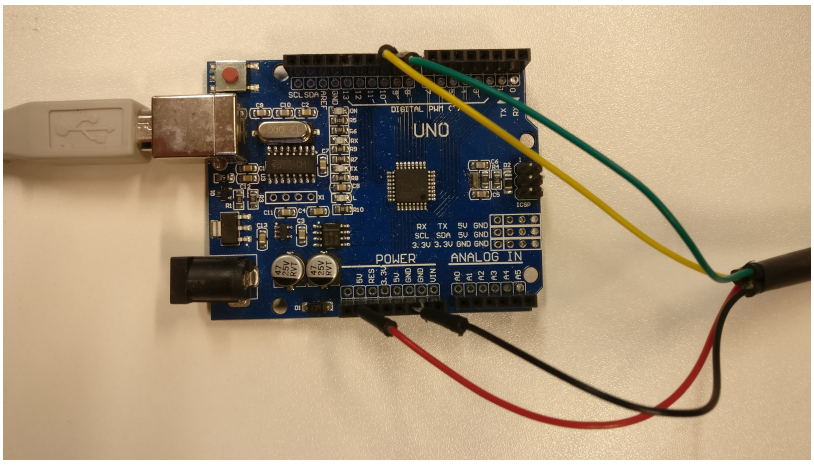

Figure 22: Picture of the Arduino Uno micro controller connected to the sensor is used to transfer the collected data to a computer by USB.

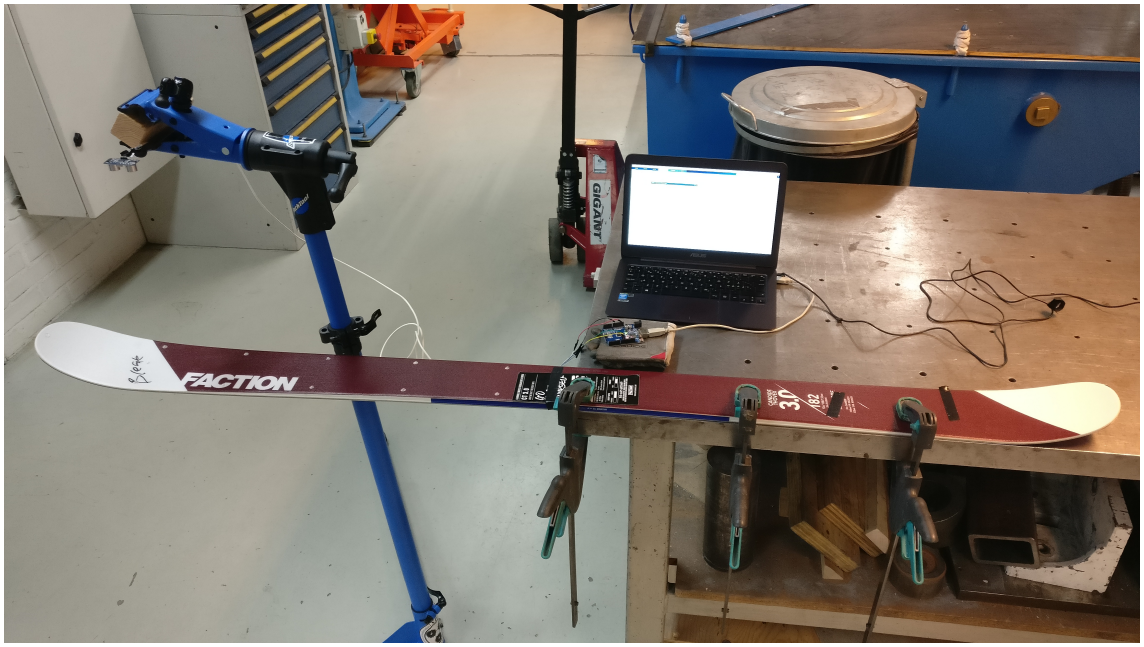

Figure 23: Picture of the setup used to conduct the simple vibrations test.

By visual inspection it was estimated that the frequency of the ski was at absolute greatest 15-20 Hz. Therefore, it was adequate to set the sample rate to 100 Hz to avoid aliasing and to also capture the nearest harmonic frequencies, if any since higher sample rates allows FFT to capture more frequencies. The number of sample points was chosen to 2^9 which gave a recording time of approximately 5 seconds, enough to capture most of the oscillation large enough to measure. The test was conducted 10 times. It was also filmed once in slow motion, from which the number of periods in a second was counted manually to confirm that the FFT produced the correct result.

3.7.1.2 Sources of error

There are two sources to jitter that could make the sample rate deviate and obscure the data. These are the times it takes to run the code and the time it takes for the sensor to retrieve it's pulse. The cycle time for the code was measured using the Arduino library's function to measure micro seconds (*Arduino*, 2018). The loop time was found to deviate at most by 30 micro seconds from 0.01 seconds (100 Hz), that is an error of 0.3 %, small enough not to affect the results.

The time it takes for the sound waves to travel back and fourth between the sensor and ski is of greater concern. By the nature of the sensor, the measurement time will vary from when the ski is nearest to the sensor compared to when it's furthest away. As the ratio between these times is further from one, FFT will falsely identify a larger amplitude for other frequencies, a higher noise level. If the oscillation has an amplitude of maximum 5 cm (which the sound travels twice) and the speed of sounds is 343 m/s, the maximum timing error can be calculated as follows

$$error = \frac{variation\ time}{total\ time} = \frac{2 * \Delta distance/speedofsound}{sample\ interval} = \frac{2 * 0.05/343}{0.01} = 3\% \tag{28}$$

A timing error of 3 % is generally significant in signal analysis but will not prevent finding the primary frequencies of the system.

Another source of error can be seen in the data, see Figure 37. Some data points are significantly higher than the surrounding, suggesting a faulty reading by the sensor. This would also create a higher noise level, but as can be seen in the analysis, not prevent finding the primary frequency of the system.

3.7.1.3 Legitimacy

It can be questioned to what extent the environment influences the behaviour of the ski and thus the result of the test. In contrast to the test described in Subsection 3.7.2 which aimed to isolate the system with the use of rubber balls, this test aims to imitate reality by securing the system to a point in the environment. Energy will thus be transmitted from the ski to the welding table and away. For this reason the result of this test should never be viewed as representing the ski as an isolated system.

During the project it was discovered that this method of determining dynamic properties of skis is almost identical to a standard developed by the industry in 1980 (ISO 6267:1980(en), 1980). The standard calls for a clamping device consisting of three clamps holding the ski at boot center and backwards, to a mass of at least 100 kg. This is identical to the set up used during this project. The standard also calls for an inductive transducer for taking measures with and to only analyze vibrations with an amplitude of 2 mm or smaller. This is in contrast to this test which utilized an ultrasonic sensor and analyzed vibrations with amplitudes as large as 40 mm. The existence of the standard proves that the principles of the test described in this report are sound but should be changed to fit the ISO standard before working further with it.

3.7.2 Experimental modal analysis

A second approach to measure the ski's dynamical properties was made with equipment provided by Chalmers made specifically to conduct a modal analysis with, the theory of which is described in Section 2.4.

The test was performed as follows. The ski was balanced upon three rubber supports, see Figure 24 and 25, so that the ski could vibrate freely and with as little influence from it's surroundings as possible.

Figure 24: The rubber balls used to isolate the ski during the vibrations analysis.

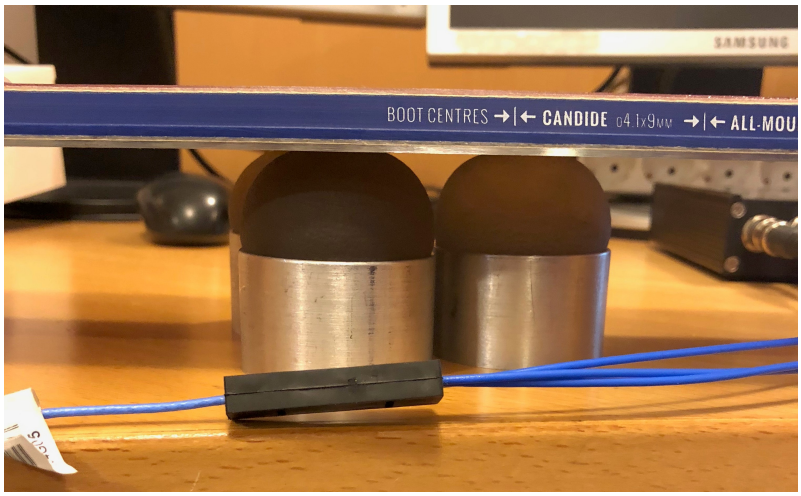

Figure 25: Placement of ski on isolating rubber balls.

An accelerometer, Figure 27a, was used to measure movement in all three directions and was placed beneath the tip of the ski. To make the ski vibrate it was hit with an impact hammer, Figure 27b. To make sure that the ski was hit at the intended positions each time, small plastic markers were placed on 12 positions across the ski. In this test, markers were placed only on the front part of the ski. More measuring positions along the ski might be of interest to further investigate vibration properties in the future. To produce data the ski was hit five times on each marker, seen in Figure 26.

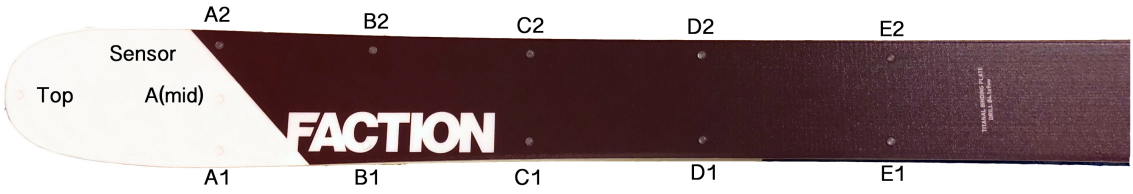

Figure 26: 12 measure positions for vibration test numbered along the ski.

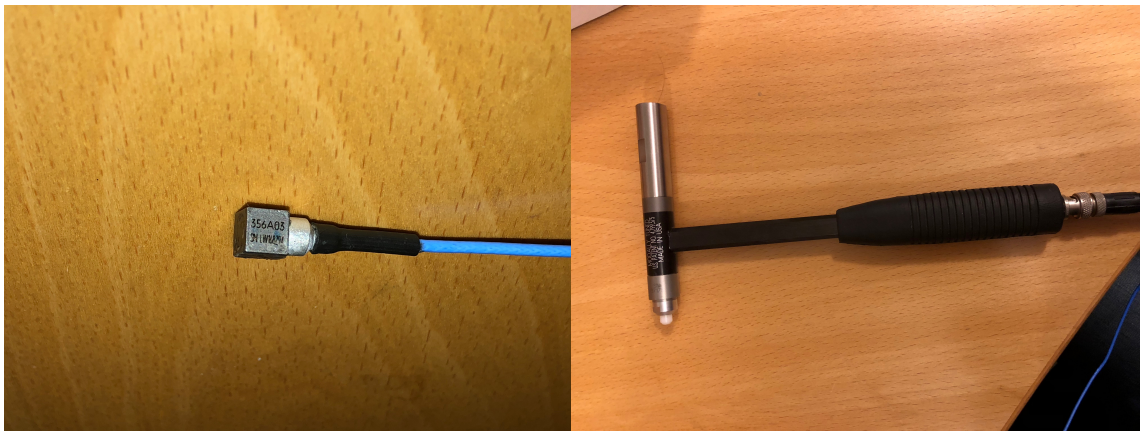

(a) Accelerometer **(b)** Impact hammer

Figure 27: Equipment for measuring vibrations.

Both the hammer and the accelerometer were connected to a data acquisition system DT9837A produced by DataTranslation, Figure 28, which in turn was connected to a PC where the output data was stored as arrays in MATLAB. Using the identification toolbox (Mathworks Inc., 2018), each collection of five tests was averaged into one result for the position in question.

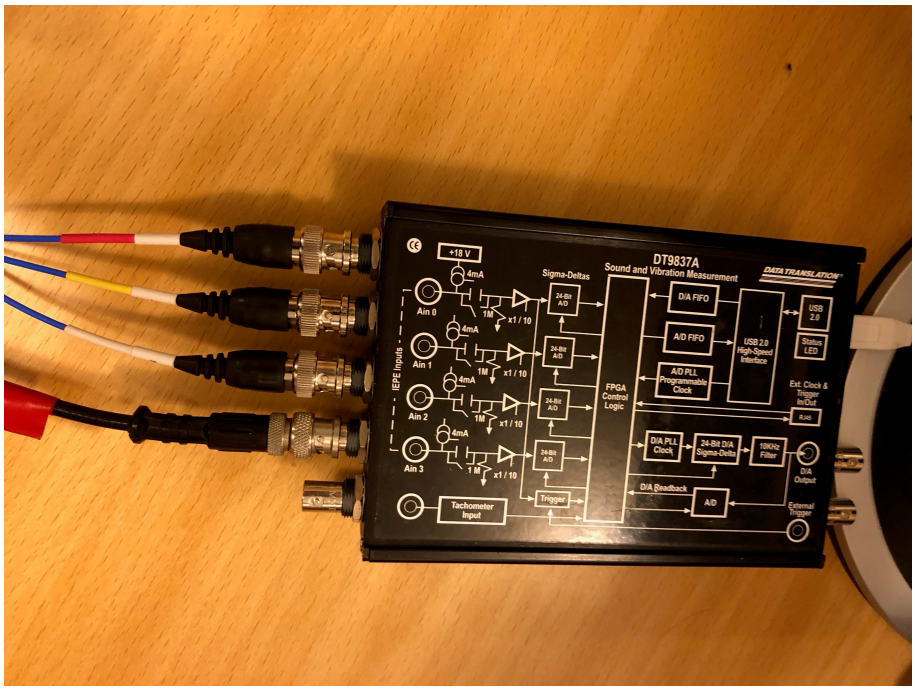

Figure 28: A picture showing the data acquisition system used to capture the skis vibrations.

System identification was then carried out using the data for the 12 nodes. Looking

at the data, the order necessary to represent the system was estimated to be in the range 18 to 30 (to capture all the major eigenfrequencies). A suitable number was found to be 24, where the model produced results close to the measures and matched most of the eigenfrequencies visible in the data. A comparison between the generated model and the measurements can be seen in Figure 29.

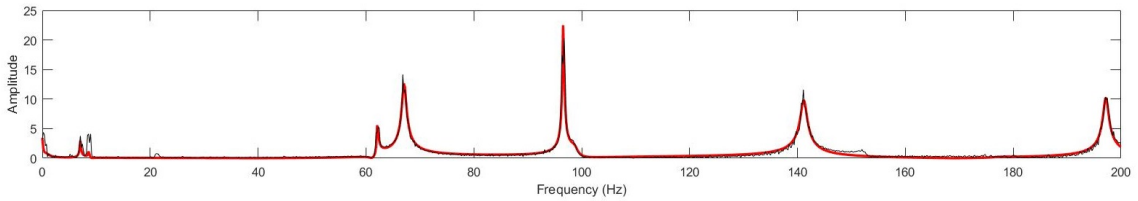

Figure 29: The identified system. Measurements are seen in black and the model is seen in red.

3.7.3 Implementation of modal vibrations in ski model

Just as for static mechanical properties such as the bending stiffness, it would be of great value to be able to model the dynamical properties of a new ski as discussed in Chapter 1. ANSYS provides tools such as it's Modal toolbox to determine the modal frequencies (eigenfrequencies) of models. It is important to note that without sufficient data on the materials' damping properties it is not possible to to find either the damping coefficient or the damped eigenfrequency for the whole ski. Only the natural eigenfrequency can be obtained, which is derived from density, elastic and geometric properties alone. However, for an under damped system, the natural and damped frequencies are very close to each other, see Equation 25.

The modal test was performed on the model with the ski constrained similarly to the two physical vibration tests. The first simulation with the ski locked in the horizontal plane and free in the vertical, imitating the ski on the rubber balls. A second simulation was made with the ski locked in all directions from the boot center and backwards but free from the tip and forwards, imitating the cantilever set up of the simple vibration test.

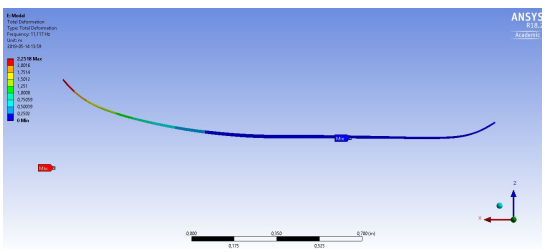

Figure 30: Picture showing first end-point of the first vibration mode.

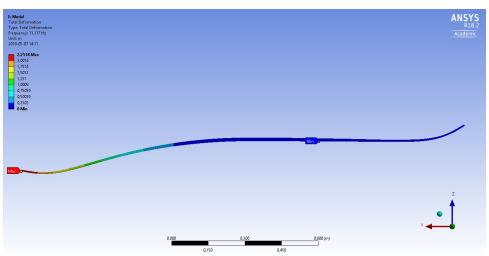

Figure 31: Picture showing second end-point of first vibration mode.

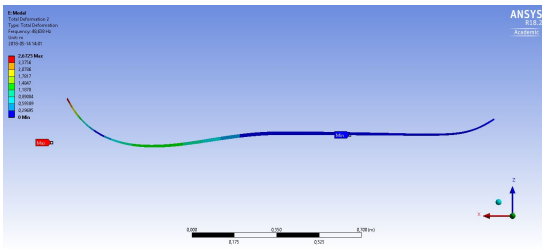

Figure 32: Picture showing first end-point of the second vibration mode.

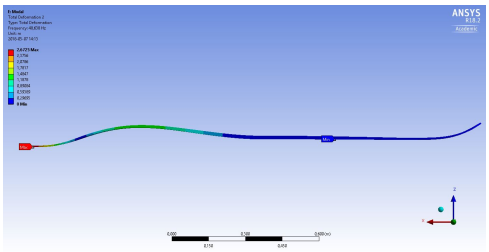

Figure 33: Picture showing second end-point of second vibration mode.

3.8 Improving ski design

The method to improve the ski design was to use the final model presented in Subsection 3.3.3 to quickly test new layups. The fact that changes in materials, fiber directions and layups can be made with great efficiency, makes it a powerful tool for quickly testing how different layups affects the mechanical properties of the ski.

The focus for the improvement part of this project was to construct a lighter ski while maintaining it's stiffness. Using the model, different lay ups was applied to see how the results in ANSYS changed. Further, discussions with Faction Skis was held to get more information on what different combinations of materials have been used in the past and how they performed. It was of importance to reflect over what was possible to model in the computer but also how manufacturable the ski would be in a factory. The information gathered during these discussion was used in moderation while improving the ski design since they were mainly focused towards the subjective feeling while skiing and not pure mechanical properties.

The first improvement lay up tried was applied with balsa in all center strips of the core and a poplar strip in line with the edge. Balsa is a lightweight but soft material (Bcomp, 2018), thus a poplar strip on the edge was inserted to protect the soft core from impacts. A proportion of the top and bottom glass fiber layers was substituted with carbon fiber, with the aim to provide a higher stiffness than the final model presented in Subsection 3.3.3 while at the same time being lighter.

The second improvement layup was applied with the same core as the first. A proportion of the glass fiber reinforcement layer under the core was substituted with Titanal. The top fabric layer was not changed compared to the final model in Subsection 3.3.3. As for improvements in damping it is impossible to tell if the damping qualities have improved or not since the model lacks constants for defining visco elastic properties. More on this will be discusses in Chapter 4.

4

Results and discussion

The data collected via the previously described methods are presented, compared and discussed in this section. These results are aimed to be the basis for continued work and improvements of the model. Discussions on how the project fits in the field of similar research and whether or not the project hypothesis is confirmed or not will also be held in this section.

4.1 Bending stiffness of final model and improved design

The eight bending tests conducted on the Candinde 3.0 produced consistent results for the load/deformation curves which can be seen in Figure 34. The results from the physical bending tests show that they follow a similar curvature with a small deviation, see Figure B.1 in Appendix B.1.

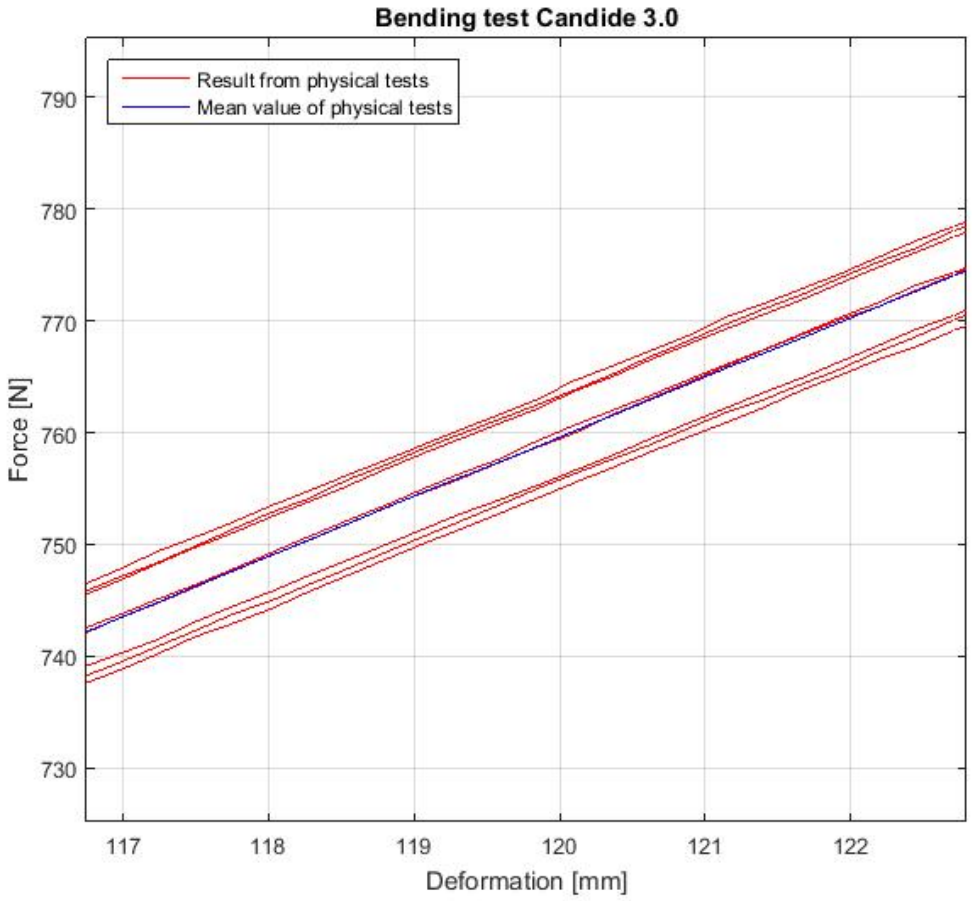

Figure 34: Plot zoomed in at 120 mm of deflection to visualize the physical test data differences.

The test rig data along with the data from the FE analysis are presented in Figure 35 which shows how much force is required to deform the ski a certain amount. As a result it is possible to visualize if and how well the model corresponds to reality.

The results seen in Figure 35 are the force/deformation plots for the physical and theoretical results from the three point bending test. The linear results in Figure 35 shows a deviation from linearity, this however was disregarded since the linear solutions are not correct for large deformations according to simple beam theory (Sundström, 2016).

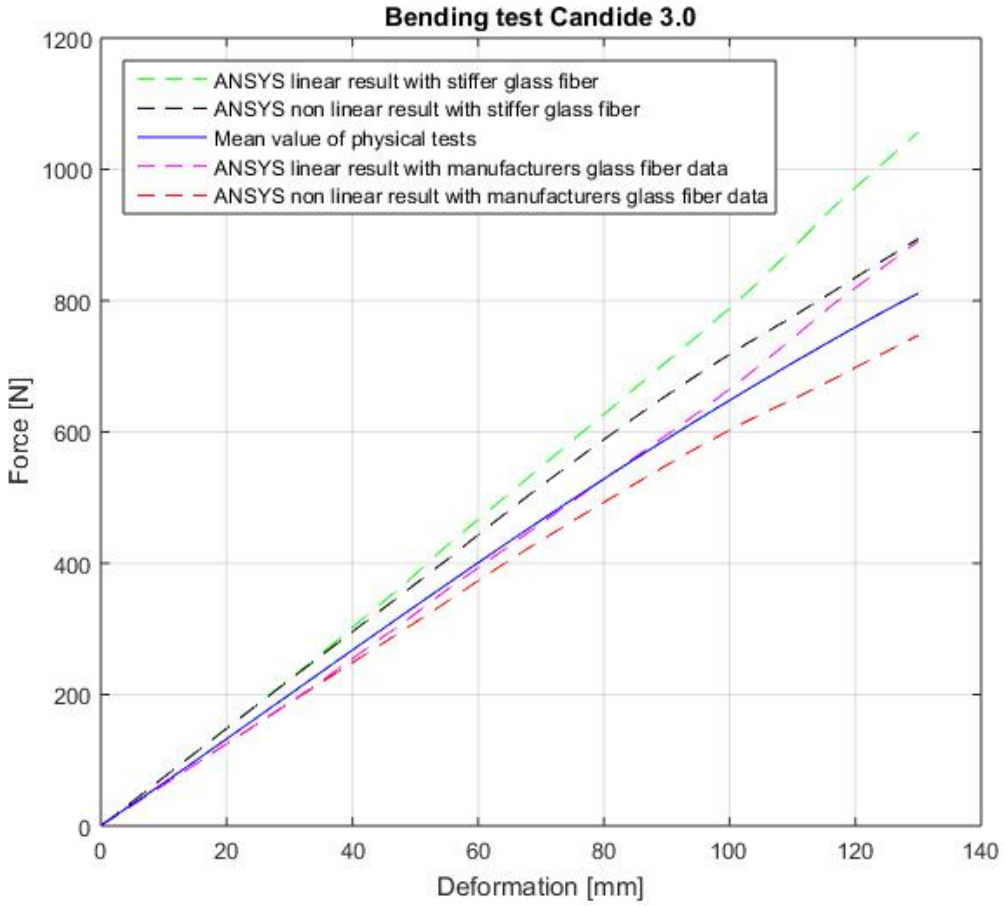

Figure 35: Plot showing the physical and theoretical results of the three point bending tests.

There was a significant difference between linear and nonlinear deformation from ca 35 mm of deflection and upwards which is in line with linear beam theory, which only works for small deflections.

The final Candide 3.0 model had a mass of 2090 g and required a 747 N to 894 N force to reach the maximum deflection of 130 mm depending on what glass fiber values used. The values correspond fairly well with the physical test data. The non linear result with stiffer glass fiber data has a mean force deviation from the mean physical test of 11.1 % while the non linear result with the manufacturer's stiffness data has a mean deviation of 7.2 %. The physical Candide 3.0 ski has a mass of ca 1850 g which is 12.9 % lower than the model weight. This is believed to be mostly due to the fact that the model is 7.7 % thicker than the actual ski (discussed in Subsection 3.3.4).

As seen in Figure 35, the results from the different glass fiber stiffness values (discussed in Subsection 3.3.4) differ from each other. A reason for why the manufac-

turer's values seem low might be that the manufacturer's sample pieces for establishing the stiffness of the glass fibre composites are containing more resin than the composites in the ski. A higher resin percentage leads to a lower stiffness since the resin is softer than the reinforcement. If the sample pieces are containing more resin it also results in thicker laminates. This is thought to be the case since the model of the ski is 1 mm (7.7 %) thicker than the physical ski when modeled with the thickness values found in the manufacturer's data.

Even though the non linear ANSYS model deviates from the actual bending stiffness it visually follows a similar non-linear response when compared to the physical testings. Therefore a continued development of the model is interesting. A reasonable first improvement of the model is to gather more accurate material data via physical tests to analyze and correct the material properties. Another way to correct the model is to test and model a large amount of skis to find out if the differences between models and actual skis are roughly the same for all skis. If this is the case, the model is reliable but not accurate and a correction factor can be implemented.

4.1.1 Improved design

The first improvement layup, with added carbon fiber (discussed in Section 3.8) is shown in Figure 36 to have an significantly improved stiffness since 1738 N is required for the said 130 mm of deflection, compared to the original 747-894 N, while having a lower weight (1840 g) than the final Candide 3.0 model which was 2090 g. This probably comes with a price of brittleness and increased vibrations, however this can not be tested in the current model since visco elastic material constants, breaking and shear strengths are not included in the model.

The second improvement layup, reinforced with Titanal shows a lower weight at around 1800g while gaining a slight increase in stiffness at 907 N for the said 130 mm of deflection. The added Titanal would probably give more desirable damping properties to the ski but this can again not be simulated due to the lack of material constants discussed in the previous paragraph.

As seen in Figure 36 both of the improvements differs from the physical ski when it comes to bending stiffness. The layup with carbon fiber's mean force deviation from the physical tests is 113.37 % while the layup with Titanal has 12.40 % mean deviation. The improved designs were compared to the Candide model with the manufacturer's stiffness data, where the design with added carbon fiber has a mean increase in force needed per millimeter of deflection of 129.63 % when compared to the Candide model, while the design with Titanal has 20.55 % mean increase in force required per millimeter of deflection from the Candide model.

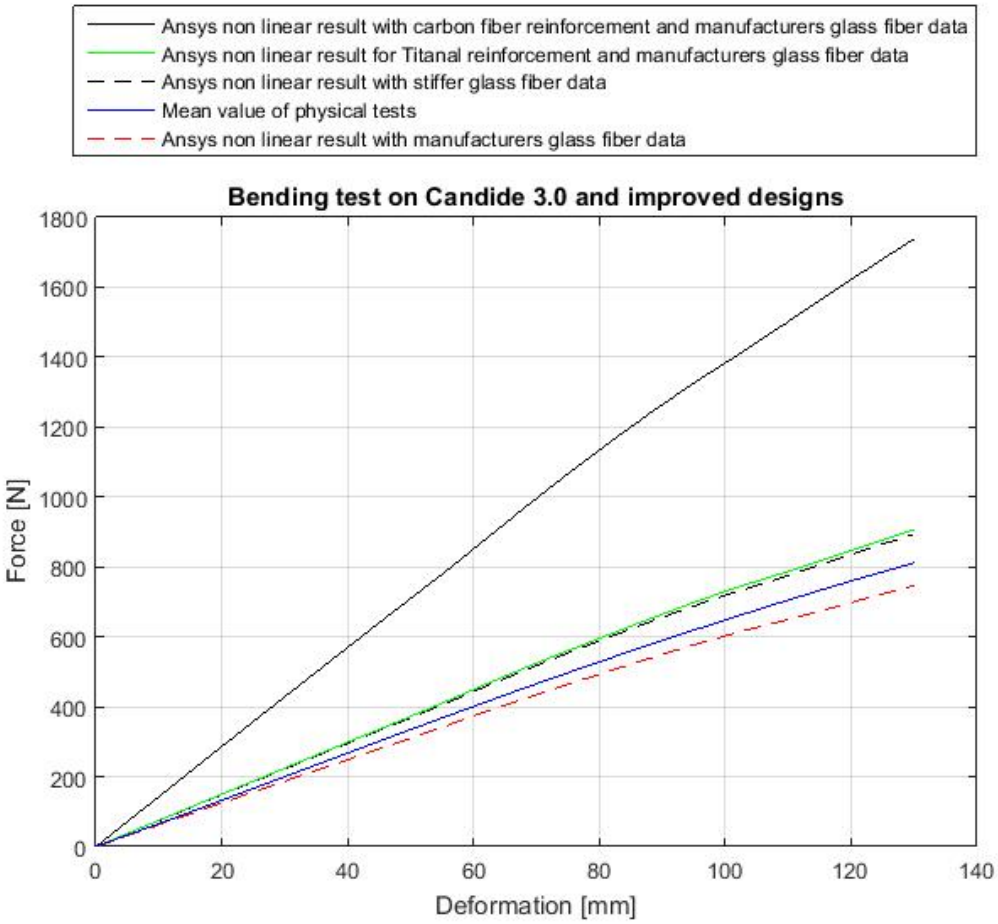

Figure 36: Graphic showing the force/deformation plot for the original and improved ski models.

4.2 Eigenfrequencies and damping coefficients

The two vibrations tests in Section 3.7 were successful in determining the eigenfrequencies and damping coefficients of their respective systems (see Subsection 4.2.1 and Table 4). It should be noted that they are not expected to correlate due to the large differences in the systems measured, described in more detail in Section 3.7.

The damping coefficients found from measurements on the whole ski could have been implemented as an average for every material in the FE model to simulate damping. But to be meaningful during future use of the model, it would be necessary to measure the damping coefficient for the individual materials of the ski. Unfortunately this was not possible during this project.

4.2.1 Simple vibration test

The fundamental eigenfrequency of the clamped Candide 3.0 ski was determined using the simple vibration test to be about 9.75 Hz. One measurement of the vibrations for the Candide 3.0 ski in the time domain as well as in the frequency domain can be seen in Figure 37. Ten overlaying samples in the frequency domain can be seen in Figure 38 which shows that the results are consistent.

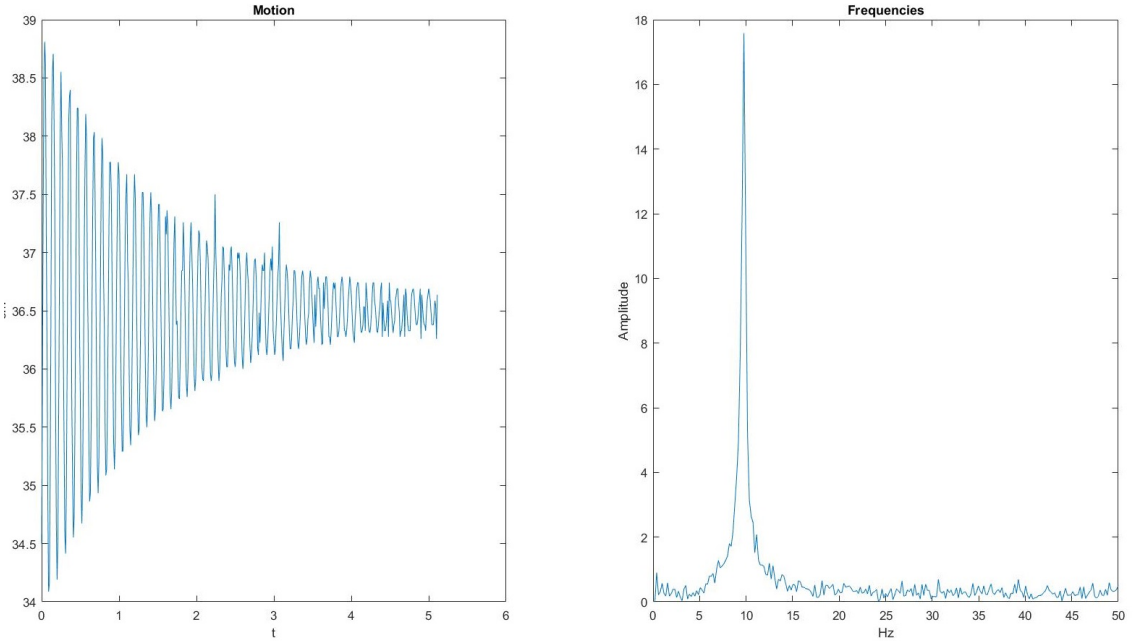

Figure 37: Two plots showing a sample of data from the simple vibration test. To the left is the motion with regards to time, to the right is the motion with regard to frequency.

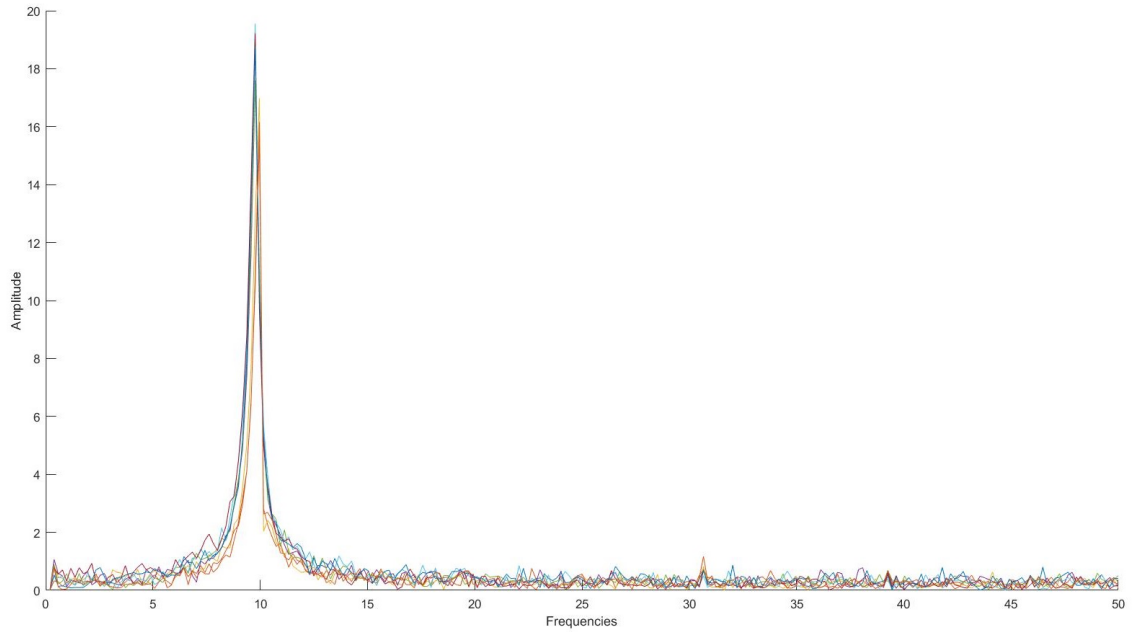

Figure 38: Ten samples of frequency data from the simple vibration test in the frequency domain.

Apart from the primary frequency at 9.75 Hz, no other frequency are clearly visible above the noise level. At closer inspection however, interesting features in the data appears. There are locations in the noise where the amplitudes of all samples align to form a tiny but clearly distinguishable peak. Three locations of these peaks are at 30.7 Hz, 39.3 Hz and 45.9 Hz. The first peak can bee seen in Figure 39 while the remaining two can bee seen in Appendix D. Calculating the mean of the samples makes them clearly visible above the noise level and can be seen in Figure 40. It is theorized that these are eigenfrequencies of the ski, although it is possible that the table or table-ski system affected the sample and a more thorough analysis would have to be done to determine this. A table of all the recordings and their measured eigenfrequencies can be viewed in Appendix C.

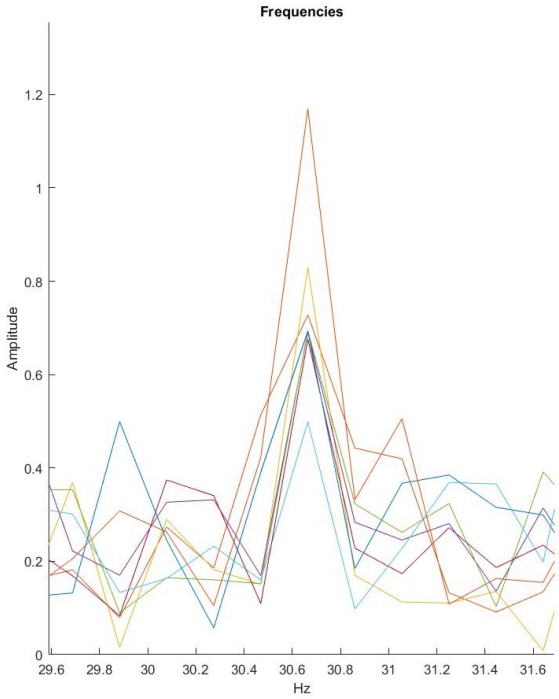

Figure 39: Plot showing amplitude spike at 30.7 Hz, thought to be an eigenfrequency.

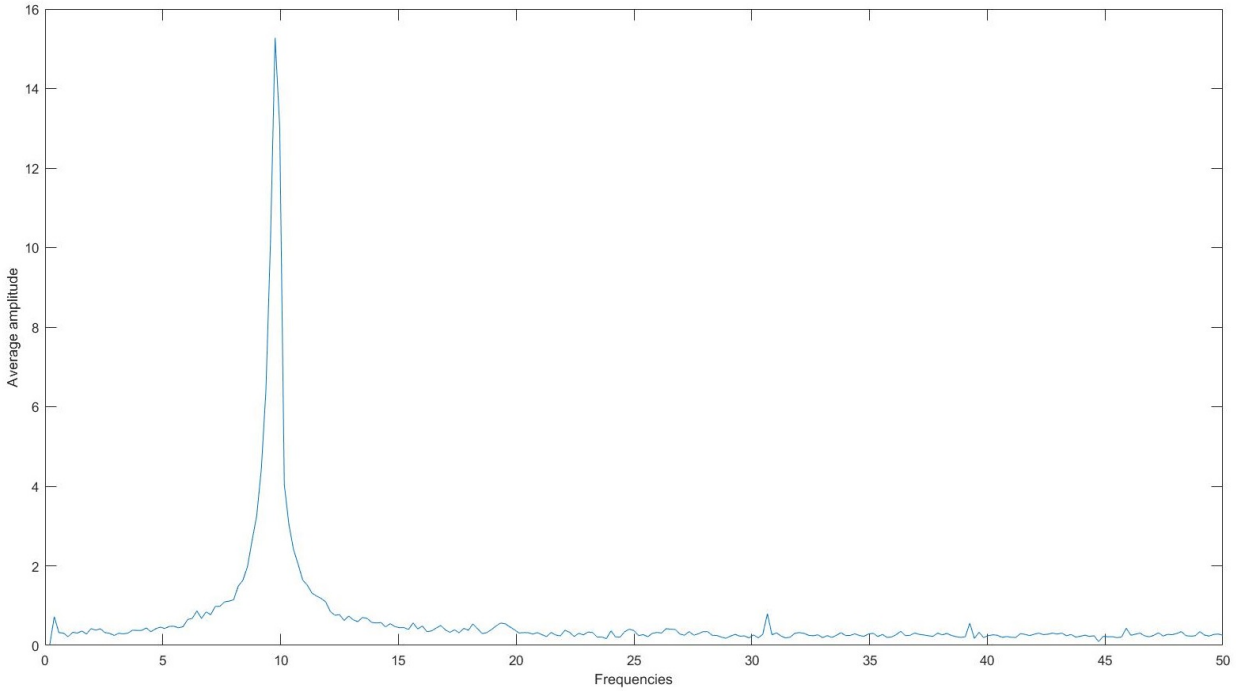

Figure 40: Plot showing the mean of all transformed vibration samples from the simple vibration test.

Using the logarithmic decrement method described in Section 2.6, the damping coefficient ζ was calculated from an average of several peaks to be approximately 0.01. These calculations are for the average of the entire sample space of eigenfrequencies although the fundamental eigenfrequency has an amplitude that is ca 15 times higher than any other eigenfrequency and hence the calculated damping coefficient of 0.01 can be viewed as the damping coefficient of the fundamental eigenfrequency. To confirm the previous statement, a mathematical model was created (see Equation 26), for the vibration using the fundamental eigenfrequency at 9.75 Hz and the damp coefficient of 0.01. The model and data from the test was plotted in Figure 41. The exact model can be seen in Equation 29. Note that the amplitude was centered around zero to adjust for the constant distance between the sensor and ski.

$$x(t) = -2.05e^{-0.01*2\pi 9.75t}cos(2\pi 9.75t) \tag{29}$$

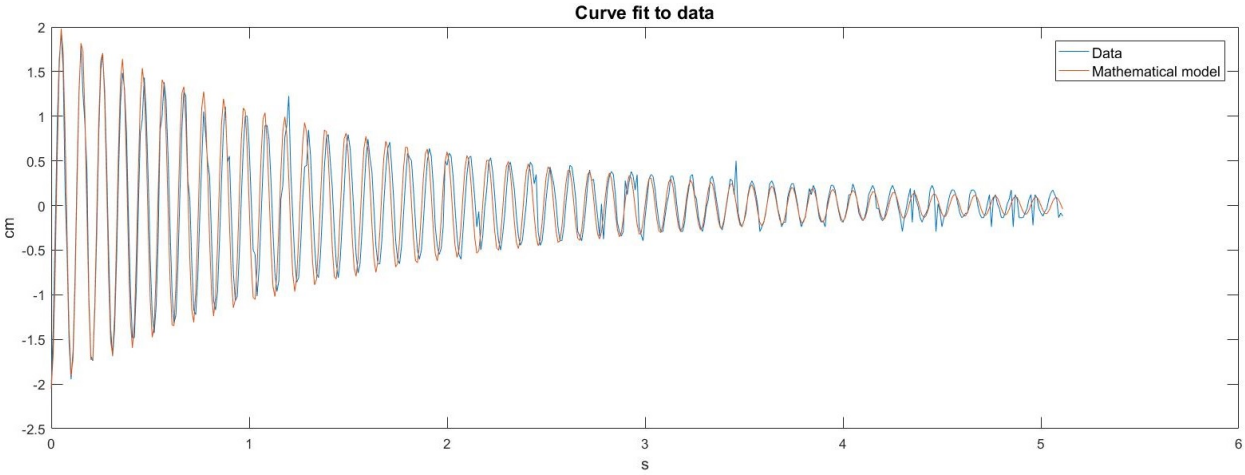

Figure 41: Plot showing a mathematical model fitted to the vibration data from the simple vibration test.

4.2.2 Experimental modal analysis

Looking at data collected using the modal analysis at points along the ski (see Figure 26), it was determined that the ski vibrated with a fundamental eigenfrequency of about 10 Hz. At closer look, it is apparent that there are actually two distinct frequencies near 10 Hz. It is believed that the lower of these two, which is at 7 Hz, is the ski oscillating on the rubber balls supporting it and that the higher at 9 Hz is the actual fundamental frequency of the ski. It is possible that this frequency at 9 Hz is the same mode that the simple vibration test found between 9 Hz and 10 Hz, see Subsection 4.2.1. At about 62 Hz and 67 Hz the first two harmonics of the vibration are found and additional ones are found at 97 Hz, 141 Hz and 197 Hz and can be seen in Figure 42.

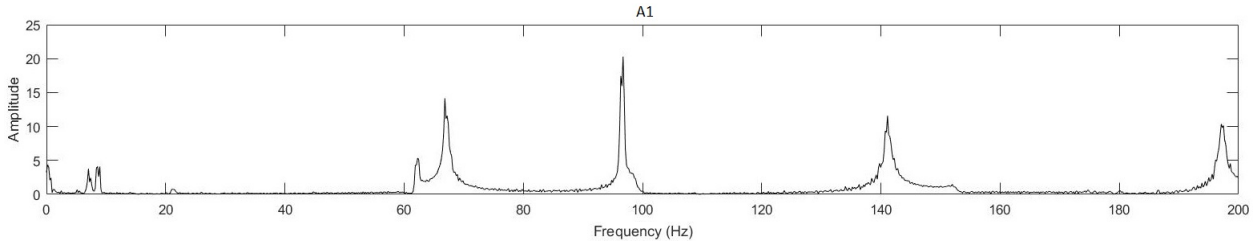

Figure 42: Frequency response of ski a measurement at position A1 using modal analysis.

The data for position "Top" (see Figure 43) is fairly similar to the data for position A1, although a large peak has appeared at 2 Hz. The theory to what causes this peak is that the ski started swinging in a seesaw motion on the support structure during this test since the impact position was right at the end of the ski. Near the boot of the ski at position D1, see Figure 44, some amplitudes have changed drastically. Compared to Position "Top", the frequency at 67 Hz is almost gone and the frequency at 141 Hz has a much stronger present. The frequency response for all points can be found in Appendix E.

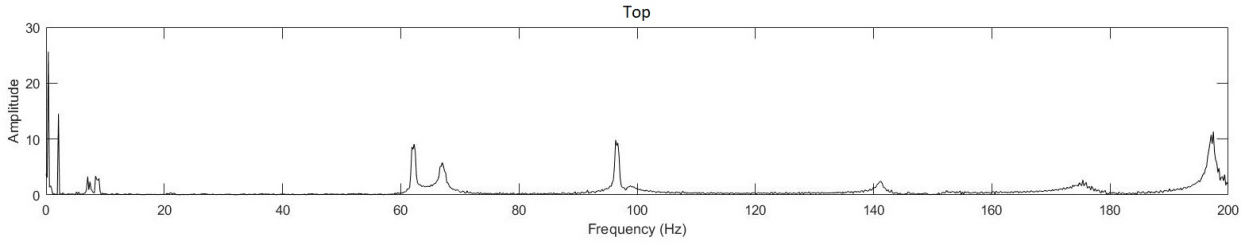

Figure 43: Frequency response of ski a measurement at position "Top" using modal analysis.

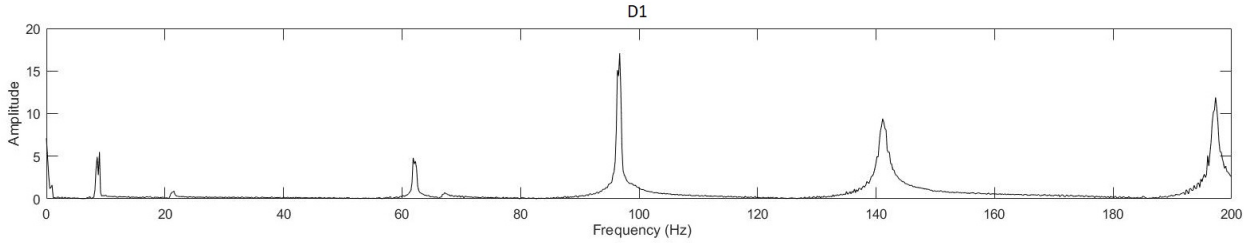

Figure 44: Frequency response of ski a measurement at position D1 using modal analysis.

From the identified system, see Figure 45, it was possible to find the damping coefficient for each of the eigenvalues using the identification toolbox (Mathworks Inc., 2018). The damping coefficients can be found in Table 4. The identified values are smaller than the value for the simple test. The reason for this is unknown.

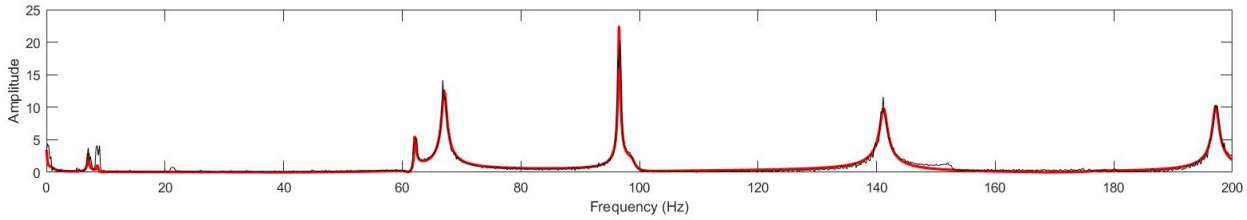

Figure 45: Frequency response of data (black) and identified system (red) for position A1.

Frequency [Hz]	Damp coefficient
9	0.0033
62	0.0017
67	0.0061
97	0.0098
141	0.0044
179	0.0130
197	0.0027

Table 4: Table showing damping coefficients found using system identification of modal analysis.

4.2.3 ANSYS modal analysis

Using the modal toolbox in ANSYS, the six first modes of the vibration and their undamped eigenfrequencies was analyzed. In Table 5 the results for material data according to Patrik Sannes (personal communication, February 6 2018) can be viewed. The results for material data according to Faction Skis manufacturer can be viewed in Table 6.

Mode	Frequency [Hz]
1	12.14
2	53.59
3	80.29
4	110.00
5	130.16
6	131.85

Table 5: Table showing eigenfrequencies found using ANSYS and Patrik Sannes (see Subsection 3.3.4) material data.

Mode	Frequncy [Hz]
1	11.12
2	48.64
3	77.36
4	106.33
5	119.62
6	126.83

Table 6: Table showing eigenfrequencies found using ANSYS and the manufacturer's material data.

The results from the modal analyses conducted on the FE model differs from the physical testings and from each other. The only difference between the two analyses made in ANSYS is the stiffness of the glass fibre. From this a conclusion can be drawn, that it is very important to determine the correct material properties before conducting an analysis in ANSYS.

4.3 Suggestions for future work

As mentioned in Chapter 1 new ski designs are often based on previous experience. With some further work towards breaking, delamination and shear strength for the model, there is a good chance that the model can help aid in the development of more eco friendly skis, since non conventional materials can be inserted into the model for verification of strength. For this application the ACP toolbox is a great tool since it has support for inter laminar stresses as well as progressive damage analysis.

FE analysis can reduce the need for physical prototypes, which in turn leads to a direct reduction in the use of epoxy and other environmentally hazardous substances during development. However, the number of skis produced as prototypes during development are small compared to the number shipped to consumers.

The model's sidewall and steel edges are simplified as a uniform square shape as seen in Subsection 3.3.3. To obtain a more life like model the sidewall should be reshaped into it's actual shape. The top sheet mentioned in Subsection 3.3.3 should also be implemented in the model.

To further increase credibility, the model could be modified to represent another ski with the same shape and design as the Candide 3.0 but another composition of materials. If the model is comparable to physical testings with satisfactory results it would further imply that the model is a trustworthy tool. This is a method used

by (Wolfsperger et al., 2016) in a project where one ski design with different layups is analyzed.

There was a plan to model another one of factions ski models: the Prodigy 4.0 to verify the model such that if both the Candide 3.0 and the Prodigy 4.0 showed a similar amount of divergence from the physical tests; the model could be corrected to show the correct stiffness. This plan however was abandoned due to the time limit.

Since skis are exposed to large temperature gradients during the season, a model which takes into consideration the materials thermal expansion could be of use while designing skis with new and non proven materials.

Another possible step to further develop this model is to quantify the definition of a good ski for different areas of skiing so that the model can be used to actually simulate and determine the performance of a ski. This would however be a completely different form of study which would greatly benefit of being combined with a study similar to this.

With the accurate material data, information about the skis' eigenfrequencies can just as easily be obtained through the FE model. If the material data includes the damping properties, the FE model could be used to predict the damping coefficient of the ski as well. The simple vibration test would be a great tool for collecting these. It could be used to determine the damping coefficient of individual materials such as the wood core and glass fiber which could then be included into the FE model. A modal analysis could also accomplish what the simple vibration test did.

5

Conclusion

To answer the main research question, a virtual ski model was created. An optimal model for the ski industry containing inter laminar stresses, partial delamination theory, breaking modes and visco elastic materials was not obtained in the thesis. However a model which is well on it's way towards the final goal was achieved with a reasonable high accuracy for both bending stiffness and eigenfrequencies.

The purpose of the thesis was to create a virtual model for ski design which could aid the ski industry by making the development process faster, cheaper and more environmental friendly. The purpose is not completed in it's entirety since to the model is lacking features due to the strict time limit of the project. The model is however on a great path to reaching a level of development where it could be used to aid the ski industry in the development of skis. If the improvement suggestions proposed in Section 4.3 are implemented the model will be a very powerful tool for ski design, especially when trying materials and layups that are not proven and new to the ski industry. The reason this is important for the continued evolution of the ski industry is that most companies are very hesitant to try new and unproven materials and layups since a failed prototype series costs both time and money.

The purpose of this project was not to model and improve properties directly connected to skiing, since skiing properties are highly subjective, but to model and improve pure mechanical properties to aid in the development process of skis. The results of the bending stiffness test and FE model analysis correlated well. With more detailed material data, very accurate results could be obtained. This makes the FE model a valuable tool for ski developers since it could quickly and cheaply predict the performance of prototype skis with different materials, shapes and layups.

The main findings in this project is that a virtual model can in fact simulate a physical ski very well, even to the point that it will be useful for the ski design process.

References

Alciatore, D., & Michael B. Histand, D. (2012). *Introduction to mechatronics and measurement systems.* McGraw-Hill.

Alpine skis — Measurement of bending vibrations (Standard). (1980, may). Geneva, CH: International Organization for Standardization.

AMAG. (2018). *Leadproduct in a wide range of high strength alloys.* Retrieved from https://www.amag.at/en/our-aluminium/sporting-consumer-products/sporting-goods/amag-titanalr.html

ANSYS Inc. (2018). *Introduction to ansys composite preppost (acp).* Retrieved from https://www.ansys.com/es-es/services/training-center/structures/introduction-to-ansys-composite-preppost

Arduino. (2018). Retrieved 2018-05-05, from https://www.arduino.cc/

Autodesk Inc. (2018). *3d cad software for product development.* Retrieved from https://www.autodesk.com/products/inventor/overview

Bcomp. (2018). *Natural fibers.* Retrieved from http://www.bcomp.ch/en/natural-fibres/balsa

Faction Skis. (2018). *About us.* Retrieved from https://factionskis.com/pages/about-us

Fagerström, M. (2018). *Lecture notes: Composite mechanics* (Tech. Rep.). Material and Computational Mechanics. Retrieved from https://pingpong.chalmers.se/courseId/9114/node.do?id=4272865&ts=1513330116560&u=847884525

Grahn, R., & Jansson. (2013). *Mekanik: statik och dynamik.* Studentlitteratur.

Granta Material Intelligence. (2018). *Cambridge engineering selector.* Retrieved from http://www.grantadesign.com/products/ces/

Intergrated, M. (2018). Retrieved from https://www.maximintegrated.com/en/app-notes/index.mvp/id/1916

James, G. (2011). *Advanced modern engineering mathematics.* Addison-Wesley.

Ljung, L. (1998). System identification. In *Signal analysis and prediction* (pp. 163–173). Boston, MA: Birkhäuser Boston.

Loos, M. R., Coelho, L. A. F., Pezzin, S. A. H., & Amico, S. C. (2008, 09). Effect of carbon nanotubes addition on the mechanical and thermal properties of epoxy matrices. *Materials Research*, *11*, 347 - 352.

Mathworks Inc. (2018). *Matlab.* Retrieved from https://se.mathworks.com/products/matlab.html

Meier, E. (2018). *The wood database.* Retrieved from `http://www.wood-database.com/`

Ottosen, N. S., & Petersson, H. (1992). *Introducation to the finite element method.* Prentice Hall.

Schwarz, B. J., & Richardson, M. H. (1999). Experimental modal analysis. *CSI Reliability week*, *35*(1), 1–12.

Skibuilders. (2018). *ski building: An overview.* Retrieved from `http://www.skibuilders.com/howto/`

Sundström, B. (2016). *Handbok och formelsamling i hållfasthetslära.* Institutionen för hållfasthetslära KTH.

Truong, J., Brousseau, C., & Desbiens, A. L. (2016). A method for measuring the bending and torsional stiffness distributions of alpine skis. *Procedia Engineering*, *147*, 394–400.

Waelzholz. (2014). Retrieved from `https://www.waelzholz-skikanten.de/en/lightweight-ski-edges-snowboard-edges.html`

Wolfsperger, F., Szabo, D., & Rhyner, H. (2016). Development of alpine skis using fe simulations. *Procedia Engineering*, *147*, 366–371.

A

MATLAB calculations for simple laminate beam

Constants

```
E = [20 72 10.9 72 20]*1e9;%Titanal, Poppel, Glass
% E = [20 20 20 20 20]*1e9;
width = 0.1;    % Width of beam
h = ([0 2 2.6 12.6 13.2 15.2]-7.2)*1e-3;  % Coordinates of layer changes
F = 600;    % Force applied
```

Stiffness Calculations

```
for i = 1:length(E)
   EI(i) =((1/3)*E(i)*(h(i+1)^3-h(i)^3)); %% EI per width
end

EI_sum = sum(EI);   % Sum of EI per unit width
EI_tot = EI_sum*width; % Sum of EI
```

Beam Calculations

```
test = (F/(3*EI_tot))*(0.5^2)*0.5^2;  % Test elementary case
disp(test)
test2 = F/(46*EI_tot);
disp(test2);
```

```
    0.0181
```

```
    0.0189
```

Test

```
a = 20e9*width*(15.2e-3)^3/12;  % Testing uniform Youngs modulus
```

B

Bending test data comparison

This appendix presents the MATLAB scripts used to compare the obtained data from ANSYS and the physical testings which results can be seen in Chapter 4.1.

B.1 MATLAB code to plot the eight physical testings of the Candide 3.0 ski

Contents

This script plots the physical testing data

```
clc
clear all
close all
format long
```

Read data from physical testing and ANSYS results for Candide 3.0

```
% 8 physical bending tests are uploaded as (deformation[mm], force[N])
```

```
candide1=dlmread('Candide 3.0 - 130mm - 1.txt','\t',1,0);
candide2=dlmread('Candide 3.0 - 130mm - 2.txt','\t',1,0);
candide3=dlmread('Candide 3.0 - 130mm - 3.txt','\t',1,0);
candide4=dlmread('Candide 3.0 - 130mm - 4.txt','\t',1,0);
candide5=dlmread('Candide 3.0 - 130mm - 5.txt','\t',1,0);
candide6=dlmread('Candide 3.0 - 130mm - 6.txt','\t',1,0);
candide7=dlmread('Candide 3.0 - 130mm - 7.txt','\t',1,0);
candide8=dlmread('Candide 3.0 - 130mm - 8.txt','\t',1,0);
```

Interpolate results between 0.01 mm to 130 mm with 500 points.

```
% Interpolate the eight physical bending stiffness tests and calculate the
% mean
x_n = linspace(0.01,130,500);
y1 = interp1(candide1(:,1),candide1(:,2),x_n);
y2 = interp1(candide2(:,1),candide2(:,2),x_n);
y3 = interp1(candide3(:,1),candide3(:,2),x_n);
y4 = interp1(candide4(:,1),candide4(:,2),x_n);
y5 = interp1(candide5(:,1),candide5(:,2),x_n);
y6 = interp1(candide6(:,1),candide6(:,2),x_n);
y7 = interp1(candide7(:,1),candide7(:,2),x_n);
y8 = interp1(candide8(:,1),candide8(:,2),x_n);

for i = 1:500
    y_medel(i) = (y1(i) + y2(i) + y3(i) + y4(i) + y5(i)...
        + y6(i) + y7(i) + y8(i))/8;
end
```

Plot results

```
p1 = plot(x_n,y1,'r');

hold on
plot(x_n,y2,'r');

hold on
plot(x_n,y3,'r');

hold on
plot(x_n,y4,'r');
```

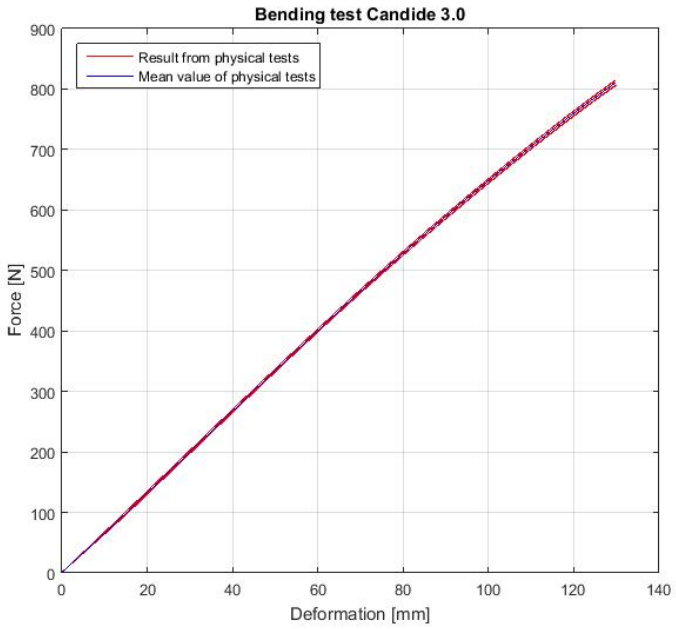

Figure B.1: Plot showing eight physical bending tests on the Candide 3.0 and their mean value.

```
hold on
plot(x_n,y5,'r');

hold on
plot(x_n,y6,'r');

hold on
plot(x_n,y7,'r');

hold on
plot(x_n,y8,'r');

hold on
p_mean = plot(x_n,y_medel,'b');

legend([p1 p_mean],{'Result from physical tests','Mean value of physical tests'},'L
ylabel('Force [N]')
xlabel('Deformation [mm]')
title('Bending test Candide 3.0')
grid on
```

B.2 MATLAB code to plot and compare physical tesing with ANSYS result for the Candide 3.0 ski

Contents

- Read data from physical testing and ANSYS results for Candide 3.0
- Interpolate results between 0.01 mm to 130 mm with 500 points.
- Plot results
- Test difference for non linear result

```
%%This script plots and compare ANSYS result for the Candide 3.0 with the physical
clc
clear all
close all
format long
```

Read data from physical testing and ANSYS results for Candide 3.0

```
% 8 physical bending tests are uploaded as (deformation[mm], force[N])
candide1=dlmread('Candide 3.0 - 130mm - 1.txt','\t',1,0);
candide2=dlmread('Candide 3.0 - 130mm - 2.txt','\t',1,0);
candide3=dlmread('Candide 3.0 - 130mm - 3.txt','\t',1,0);
candide4=dlmread('Candide 3.0 - 130mm - 4.txt','\t',1,0);
candide5=dlmread('Candide 3.0 - 130mm - 5.txt','\t',1,0);
candide6=dlmread('Candide 3.0 - 130mm - 6.txt','\t',1,0);
candide7=dlmread('Candide 3.0 - 130mm - 7.txt','\t',1,0);
candide8=dlmread('Candide 3.0 - 130mm - 8.txt','\t',1,0);

% The result (linear and non linear) from ANSYS is uploaded as
% (deformation [m], force[-N])
linj_data = dlmread('load_deformation_ansys_candide_4_lin.txt','\t',1,3);
nonlinj_data = dlmread('load_deformation_ansys_candide_4_non.txt','\t',1,3);
nonlinj_data_manu = dlmread('load_deformation_ansys_candide_5_non_manu.txt','\t',1,
linj_data_manu = dlmread('load_deformation_ansys_candide_5_lin_manu.txt','\t',1,3);
```

Interpolate results between 0.01 mm to 130 mm with 500 points.

```
% Interpolate the eight physical bending stiffness tests and calculate the
% mean
x_n = linspace(0.01,130,500);
y1 = interp1(candide1(:,1),candide1(:,2),x_n);
y2 = interp1(candide2(:,1),candide2(:,2),x_n);
y3 = interp1(candide3(:,1),candide3(:,2),x_n);
y4 = interp1(candide4(:,1),candide4(:,2),x_n);
y5 = interp1(candide5(:,1),candide5(:,2),x_n);
y6 = interp1(candide6(:,1),candide6(:,2),x_n);
y7 = interp1(candide7(:,1),candide7(:,2),x_n);
y8 = interp1(candide8(:,1),candide8(:,2),x_n);

for i = 1:500
    y_medel(i) = (y1(i) + y2(i) + y3(i) + y4(i) + y5(i)...
        + y6(i) + y7(i) + y8(i))/8;
end

% Interpolate ANSYS results
x_n_nonlinj = x_n;
y_linj = interp1(linj_data(:,1)*1000,linj_data(:,2)*-1,x_n);
y_nonlinj = interp1(nonlinj_data(:,1)*1000,nonlinj_data(:,2)*-1,x_n_nonlinj);
y_nonlinj_manu = interp1(nonlinj_data_manu(:,1)*1000,nonlinj_data_manu(:,2)*-1,x_n_
y_linj_manu = interp1(linj_data_manu(:,1)*1000,linj_data_manu(:,2)*-1,x_n);
```

Plot results

```
p_linj = plot(x_n,y_linj,'g--');
hold on

p_nonlinj = plot(x_n_nonlinj,y_nonlinj,'k--');
hold on
p_manu_nonlinj = plot(x_n_nonlinj,y_nonlinj_manu,'r--');

hold on
p_manu_linj = plot(x_n,y_linj_manu,'m--');

hold on
p_mean = plot(x_n,y_medel,'b');

legend([p_linj p_nonlinj p_mean p_manu_linj p_manu_nonlinj],{'ANSYS linear result w
```

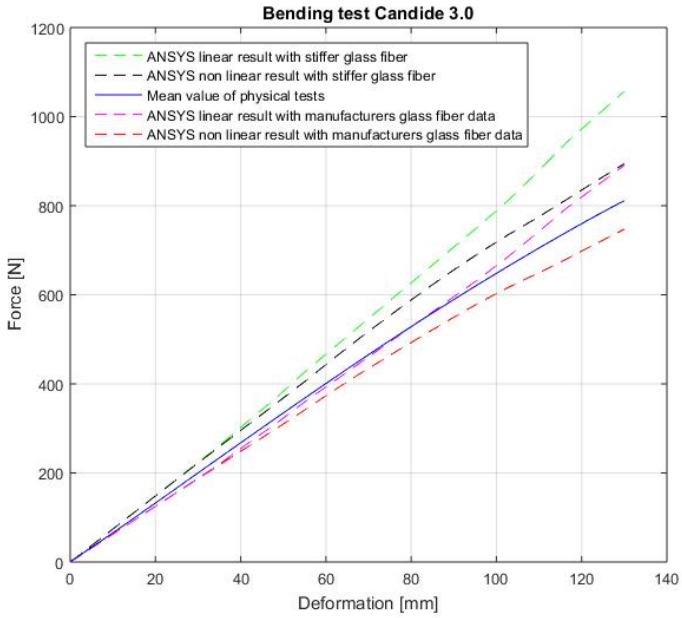

Figure B.2: Plot showing bending test results from ANSYS result and the mean result from the physical testings.

```
ylabel('Force [N]')
xlabel('Deformation [mm]')
title('Bending test Candide 3.0')
grid on
```

Test difference for non linear result

```
% With stiffer glass fiber data
for i = 1:length(x_n_nonlinj)
    diff(i) = (abs(y_medel(i)-y_nonlinj(i)))/abs(y_medel(i));
end
diff_medel = sum(diff)/length(diff)

% With manufacturers glass fiber data
for i = 1:length(x_n_nonlinj)
    diff_manu(i) = (abs(y_medel(i)-y_nonlinj_manu(i)))/abs(y_medel(i));
end
diff_medel_manu = sum(diff_manu)/length(diff_manu)
```

```
diff_medel =
```

```
   0.110588295901298

diff_medel_manu =

   0.072441302313028
```

B.3 MATLAB code to plot the stiffness results from suggested designs, physical testing and original model of the Candide 3.0 ski

Contents

This script plots and compares the ANSYS result for the Candide 3.0 with the suggested designs and the physical testings

Contents

This script plots and compares the ANSYS result for the Candide 3.0 with the suggested designs and the physical testings

```
clc
clear all
close all
format long
```

Read data from physical testing and ANSYS results for Candide 3.0 and the improved design

```
% 8 physical bending tests are uploaded as (deformation[mm], force[N])
candide1=dlmread('Candide 3.0 - 130mm - 1.txt','\t',1,0);
candide2=dlmread('Candide 3.0 - 130mm - 2.txt','\t',1,0);
candide3=dlmread('Candide 3.0 - 130mm - 3.txt','\t',1,0);
candide4=dlmread('Candide 3.0 - 130mm - 4.txt','\t',1,0);
candide5=dlmread('Candide 3.0 - 130mm - 5.txt','\t',1,0);
candide6=dlmread('Candide 3.0 - 130mm - 6.txt','\t',1,0);
candide7=dlmread('Candide 3.0 - 130mm - 7.txt','\t',1,0);
candide8=dlmread('Candide 3.0 - 130mm - 8.txt','\t',1,0);

% The result (non linear) from Ansys is uploaded as
% (deformation [m], force[-N]).
nonlinj_data = dlmread('load_deformation_ansys_candide_4_non.txt','\t',1,3);

% Result with manufacturer data for component in top fabric layer. Uploaded as
% (deformation [m],force[-N]).
nonlinj_data_manu = dlmread('load_deformation_ansys_candide_5_non_manu.txt','\t',1,

% Results from suggested designs with manufacturer data for component in
% top fabric layer. Uploaded as (deformation [m],force[-N]).
non_carbon = dlmread('load_deformation_ansys_candide_6_non_carbon.txt','\t',1,3);
non_titanal = dlmread('load_deformation_ansys_candide_6_non_titanal.txt','\t',1,3);
```

Interpolate results between 0.01 mm to 130 mm with 500 points.

```
% Interpolate the eight physical bending stiffness tests and calculate the
% mean
```

X

```
x_n = linspace(0.01,130,500);
y1 = interp1(candide1(:,1),candide1(:,2),x_n);
y2 = interp1(candide2(:,1),candide2(:,2),x_n);
y3 = interp1(candide3(:,1),candide3(:,2),x_n);
y4 = interp1(candide4(:,1),candide4(:,2),x_n);
y5 = interp1(candide5(:,1),candide5(:,2),x_n);
y6 = interp1(candide6(:,1),candide6(:,2),x_n);
y7 = interp1(candide7(:,1),candide7(:,2),x_n);
y8 = interp1(candide8(:,1),candide8(:,2),x_n);

%Calculate mean
for i = 1:500
    y_mean(i) = (y1(i) + y2(i) + y3(i) + y4(i) + y5(i)...
        + y6(i) + y7(i) + y8(i))/8;
end

% Interpolate ANSYS results
x_n_nonlinj = x_n;
y_nonlinj = interp1(nonlinj_data(:,1)*1000,nonlinj_data(:,2)*-1,x_n_nonlinj);
y_nonlinj_manu = interp1(nonlinj_data_manu(:,1)*1000,nonlinj_data_manu(:,2)*-1,x_n_

y_non_carbon = interp1(non_carbon(:,1)*1000,non_carbon(:,2)*-1,x_n);
y_non_titanal = interp1(non_titanal(:,1)*1000,non_titanal(:,2)*-1,x_n);
```

Plot results

```
p_nonlinj = plot(x_n_nonlinj,y_nonlinj,'k--');

hold on
p_nonlinj_manu = plot(x_n_nonlinj,y_nonlinj_manu,'r--');

hold on
pc = plot(x_n,y_non_carbon,'k');

hold on
pt = plot(x_n,y_non_titanal,'g');

hold on
p_medel = plot(x_n,y_mean,'b');

legend([pc pt p_nonlinj p_medel p_nonlinj_manu],{'ANSYS non linear result with carb
ylabel('Force [N]')
xlabel('Deformation [mm]')
title('Bending test on Candide 3.0 and improved designs')
```

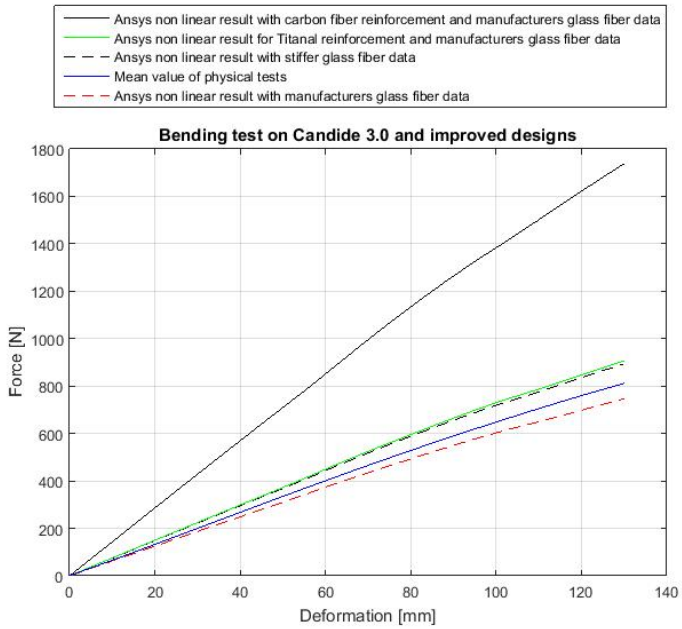

Figure B.3: Plot showing bending test results from original ANSYS model and improved designs.

```
grid on
```

```
Warning: Ignoring extra legend
entries.
```

Test difference

```
% New alternative with carbon compared to physical ski
for i = 1:length(x_n_nonlinj)
    diff_carbon(i) = (abs(y_mean(i)-y_non_carbon(i)))/abs(y_mean(i));
end
dif_mean_carbon = sum(diff_carbon)/length(diff_carbon)

% New alternative with titanal compared to physical ski
for i = 1:length(x_n_nonlinj)
    diff_titanal(i) = (abs(y_mean(i)-y_non_titanal(i)))/abs(y_mean(i));
end
diff_mean_titanal = sum(diff_titanal)/length(diff_titanal)

% New alternative with carbon compared to Candide 3.0 model with
```

```
% manufacturers data in the top sheet
for i = 1:length(x_n_nonlinj)
    diff_carbon_model(i) = (abs(y_nonlinj_manu(i)-y_non_carbon(i)))/abs(y_nonlinj_m
end
dif_mean_carbon_model = sum(diff_carbon_model)/length(diff_carbon_model)

% New alternative with titanal compared to Candide 3.0 model with
% manufacturers data in the top sheet
for i = 1:length(x_n_nonlinj)
    diff_titanal_model(i) = (abs(y_nonlinj_manu(i)-y_non_titanal(i)))/abs(y_nonlinj
end
dif_mean_titanal_model = sum(diff_titanal_model)/length(diff_titanal_model)
```

```
dif_mean_carbon =

   1.133682292179563


diff_mean_titanal =

   0.123996034456211


dif_mean_carbon_model =

   1.296266193940250


dif_mean_titanal_model =

   0.205464439847589
```

C

Data from simple vibration test

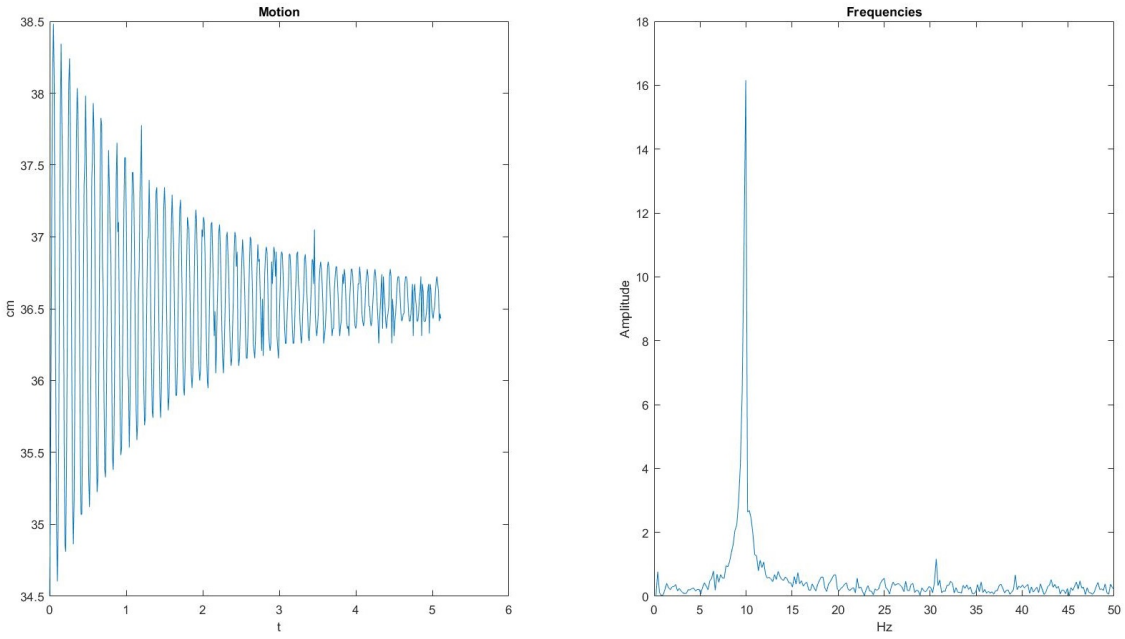

Figure C.1: Data from the first run of the simple vibration test.

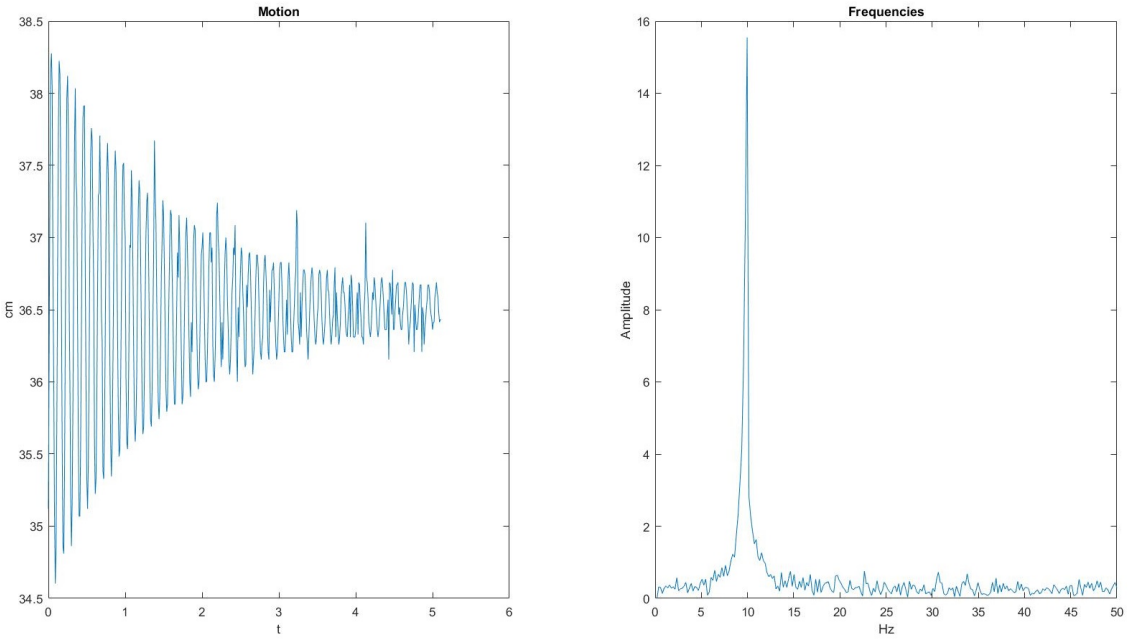

Figure C.2: Data from the second run of the simple vibration test.

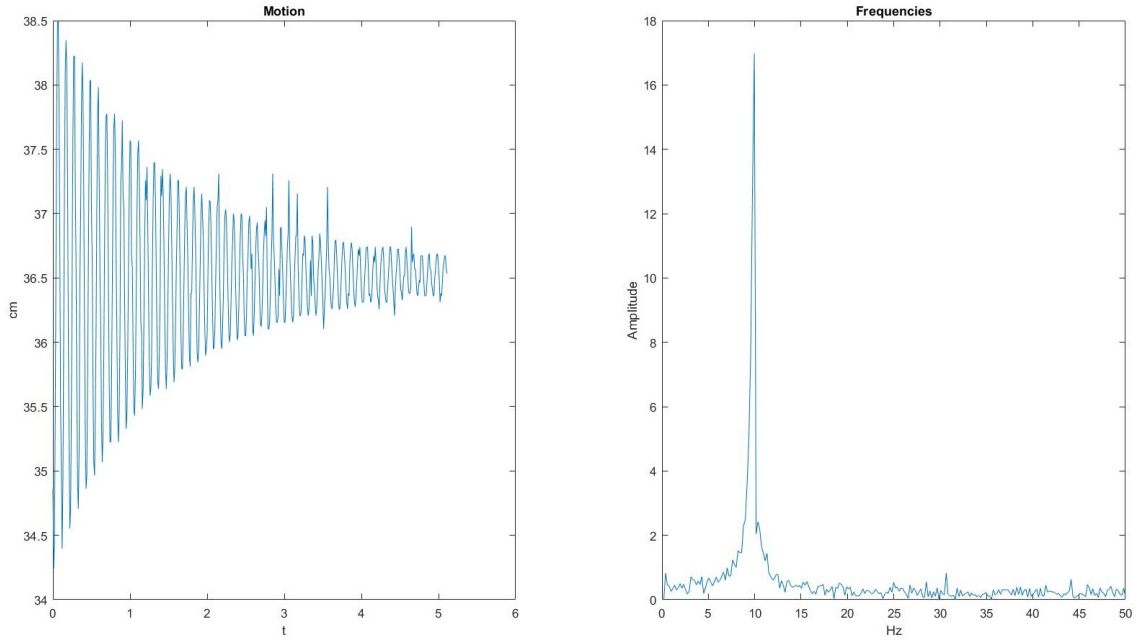

Figure C.3: Data from the third run of the simple vibration test.

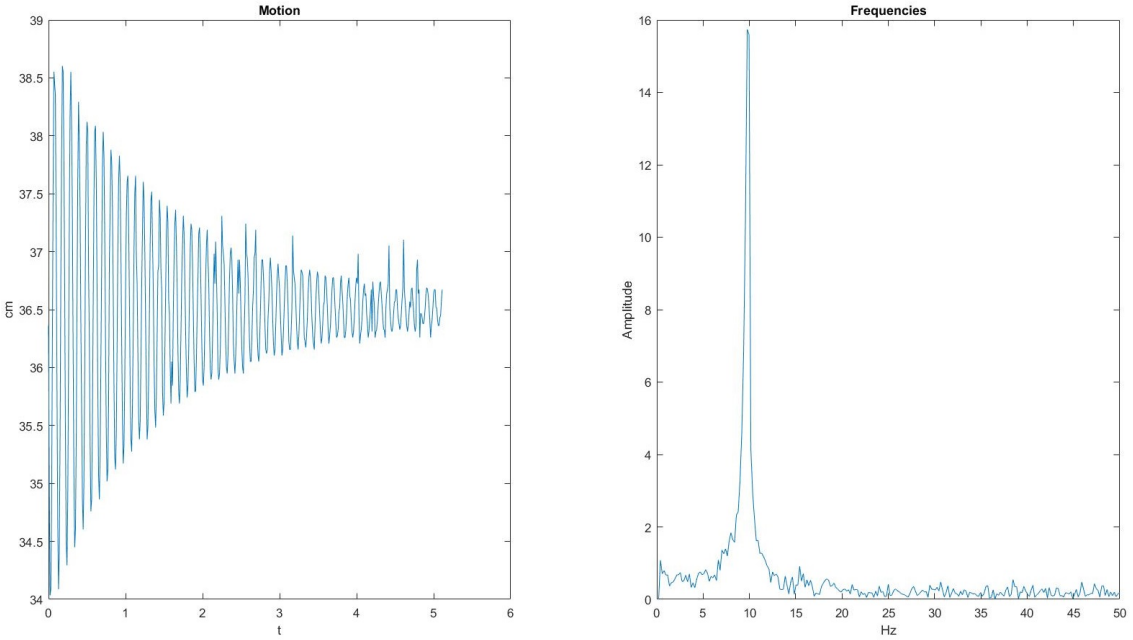

Figure C.4: Data from the fourth run of the simple vibration test.

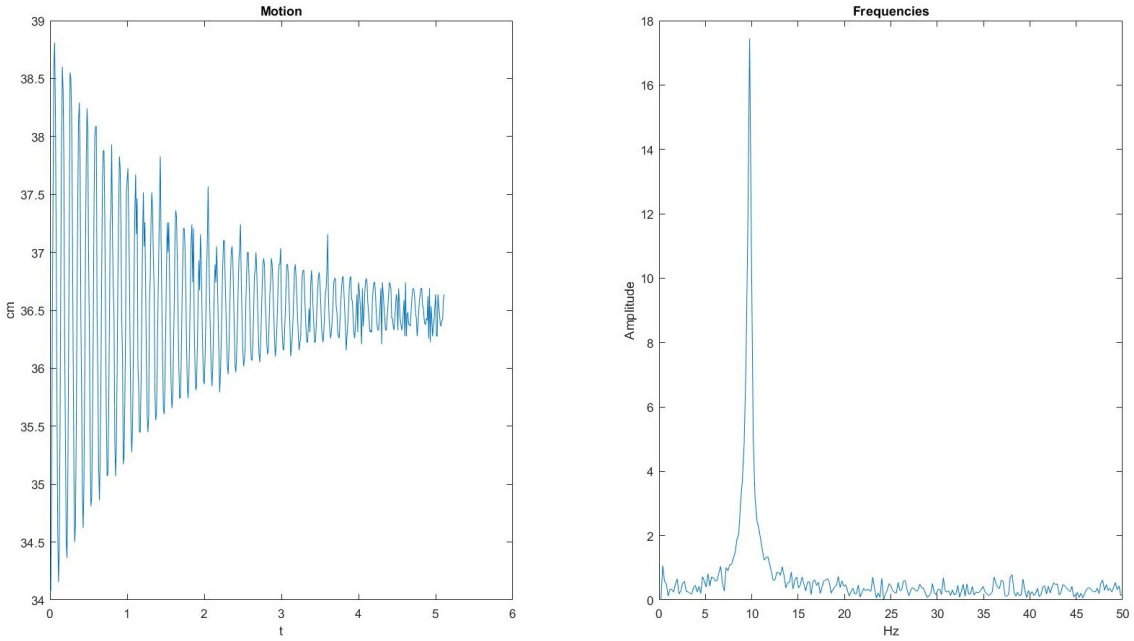

Figure C.5: Data from the fifth run of the simple vibration test.

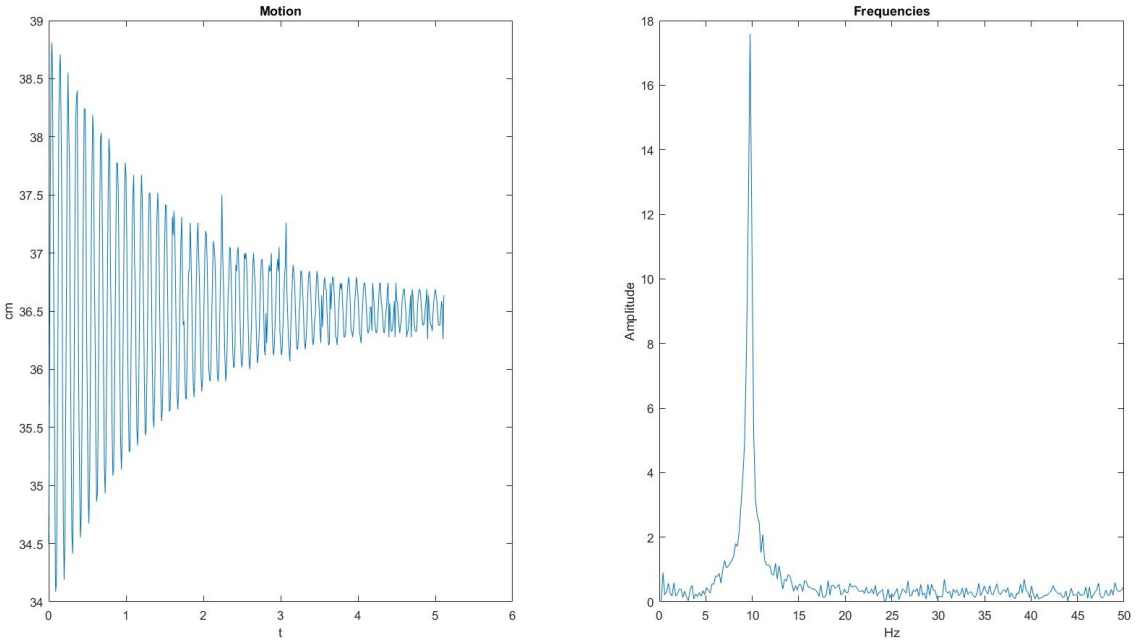

Figure C.6: Data from the sixth run of the simple vibration test.

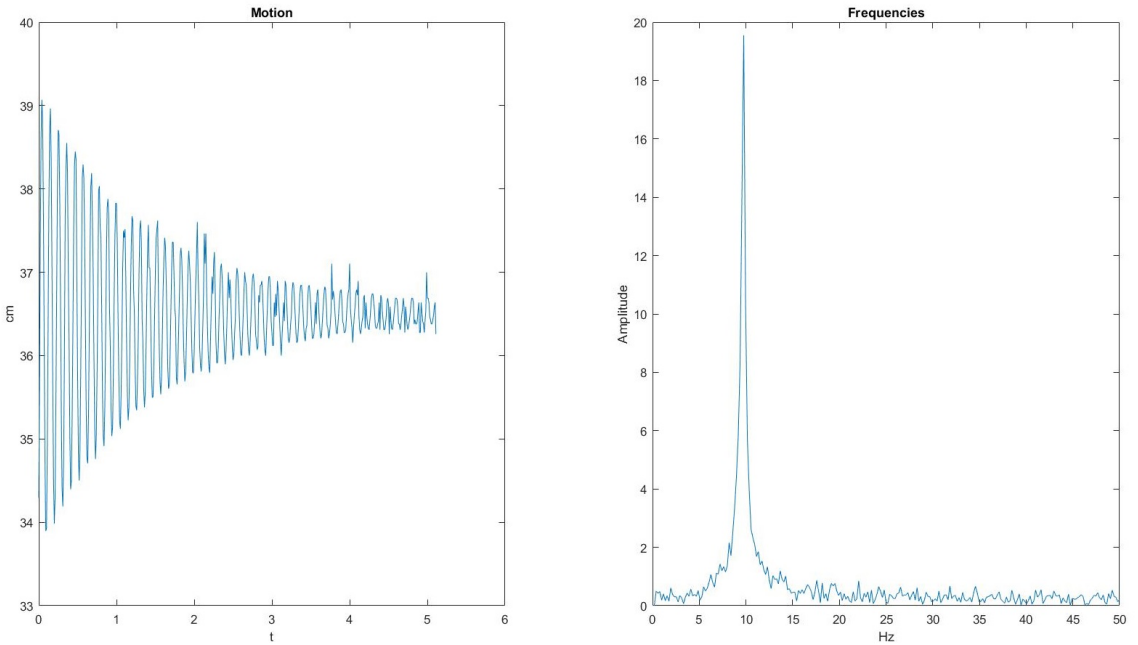

Figure C.7: Data from the seventh run of the simple vibration test.

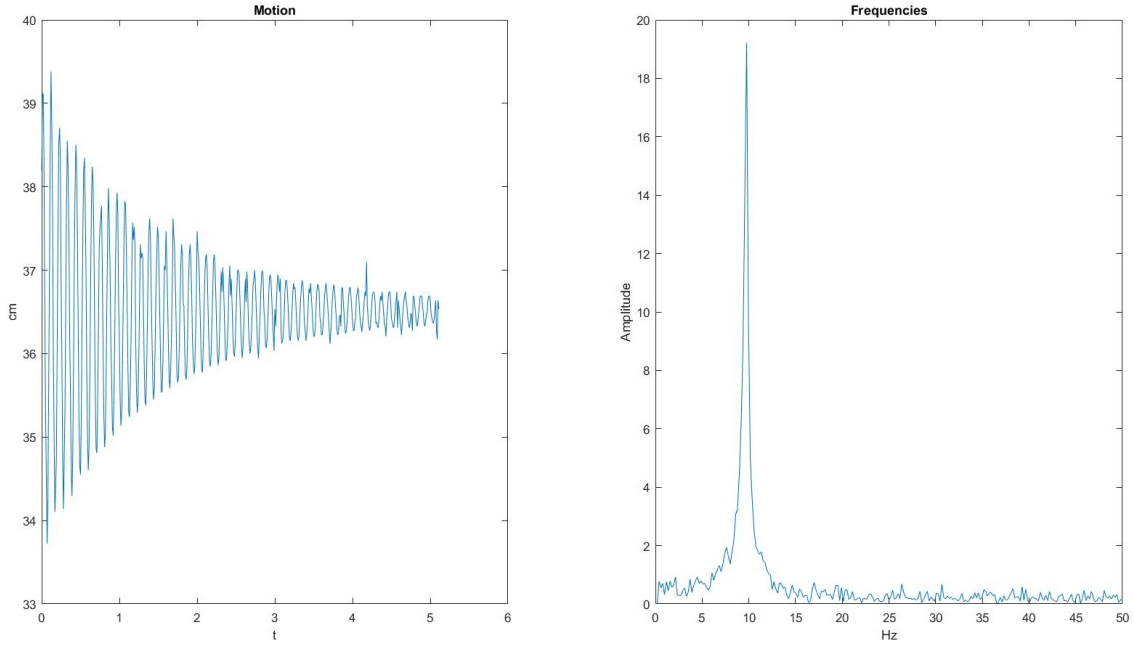

Figure C.8: Data from the eighth run of the simple vibration test.

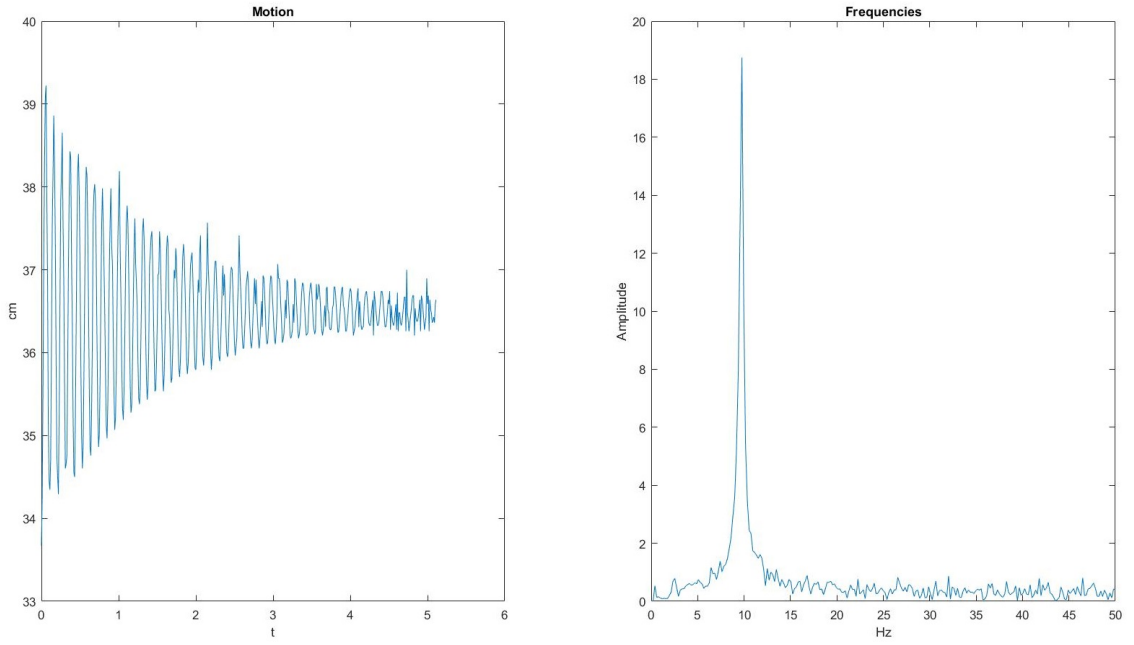

Figure C.9: Data from the ninth run of the simple vibration test.

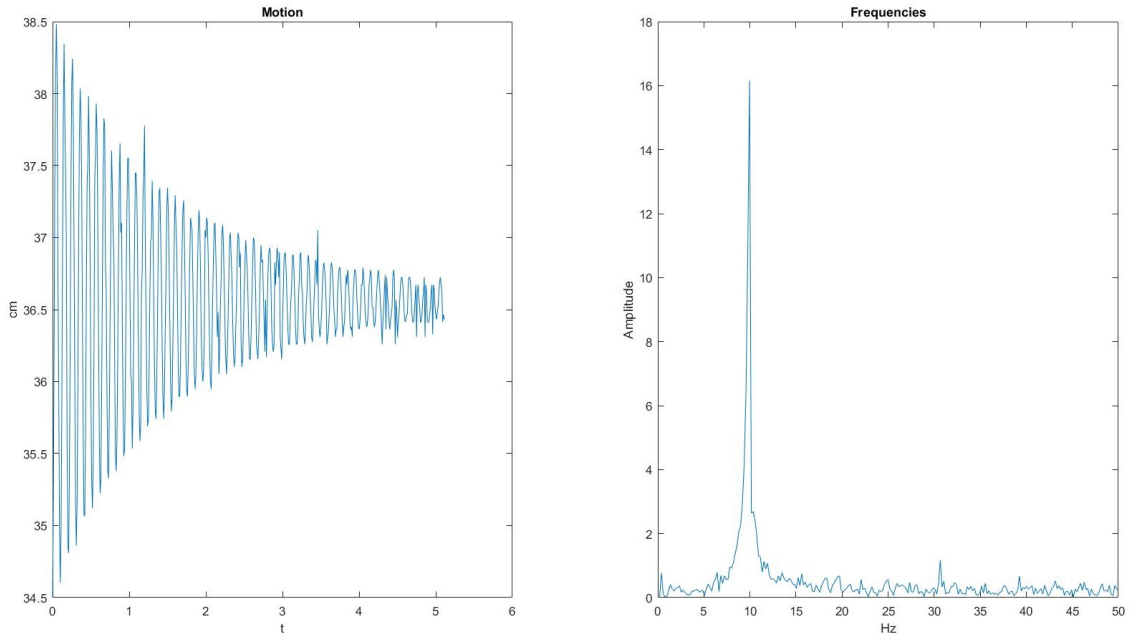

Figure C.10: Data from the tenth run of the simple vibration test.

D

Plot showing eigenfrequency amplitude spikes

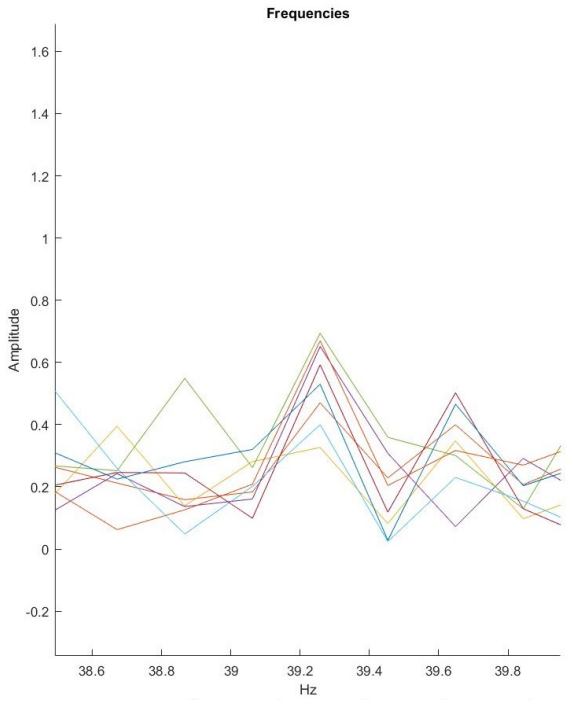

Figure D.1: An amplitude spike at 39.3 Hz thought to be an eigenfrequency.

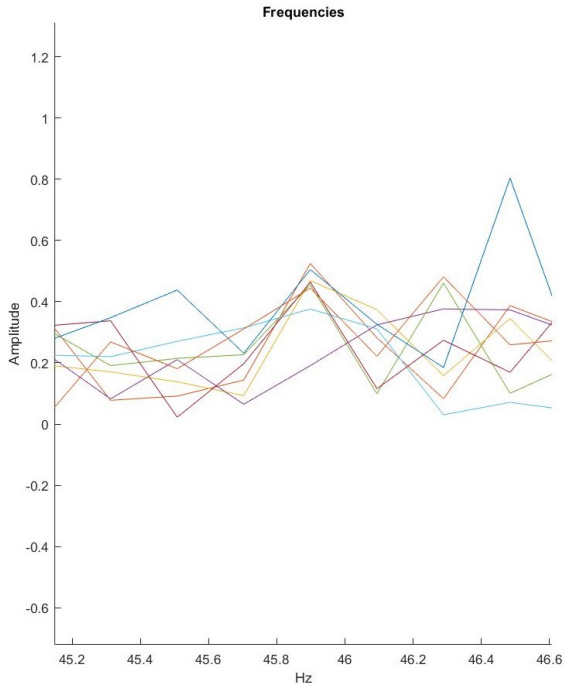

Figure D.2: An amplitude spike at 45.9 Hz thought to be an eigenfrequency.

E

Data from the modal analysis for all 12 positions along the ski

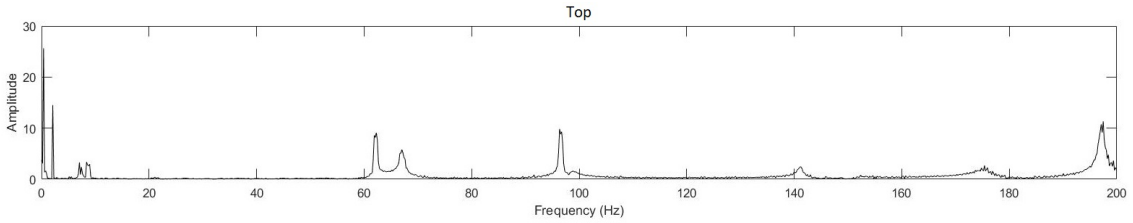

Figure E.1: Frequency response for position "Top" on the Candide 3.0 ski.

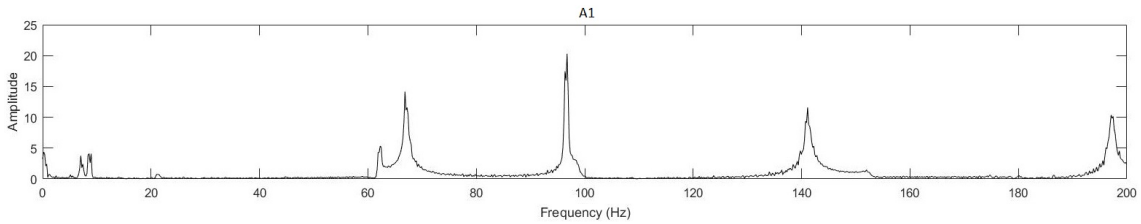

Figure E.2: Frequency response for position A1 on the Candide 3.0 ski.

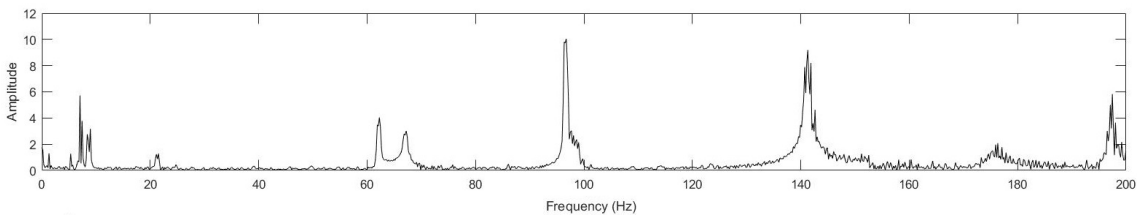

Figure E.3: Frequency response for position A-mid on the Candide 3.0 ski.

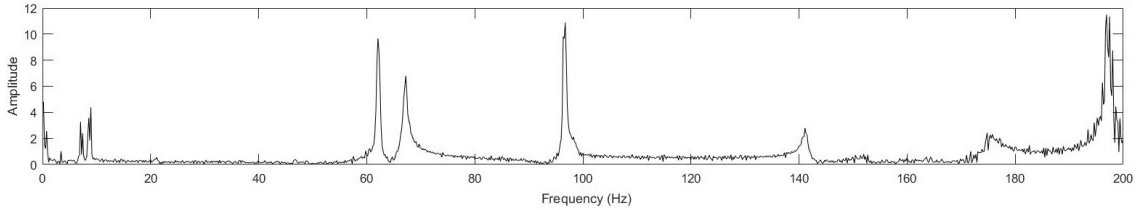

Figure E.4: Frequency response for position A2 on the Candide 3.0 ski.

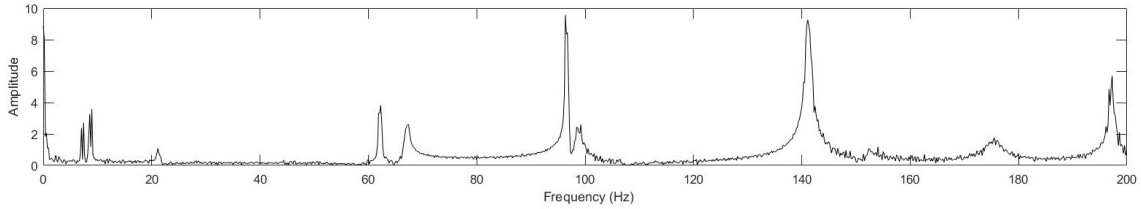

Figure E.5: Frequency response for position B1 on the Candide 3.0 ski.

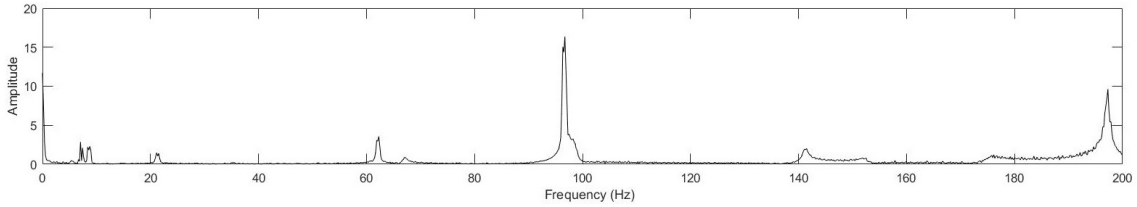

Figure E.6: Frequency response for position B2 on the Candide 3.0 ski.

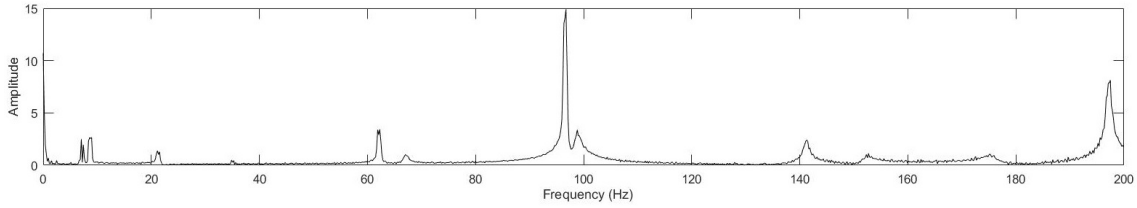

Figure E.7: Frequency response for position C1 on the Candide 3.0 ski.

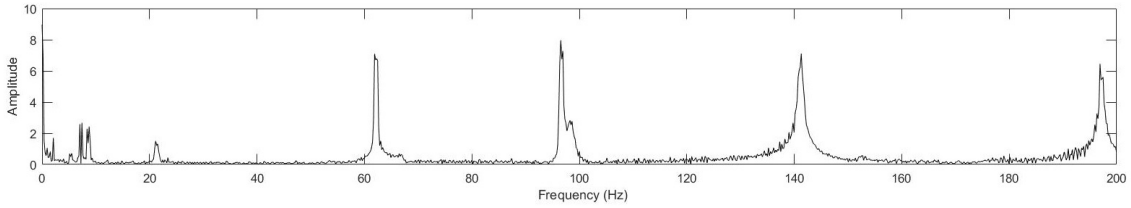

Figure E.8: Frequency response for position C2 on the Candide 3.0 ski.

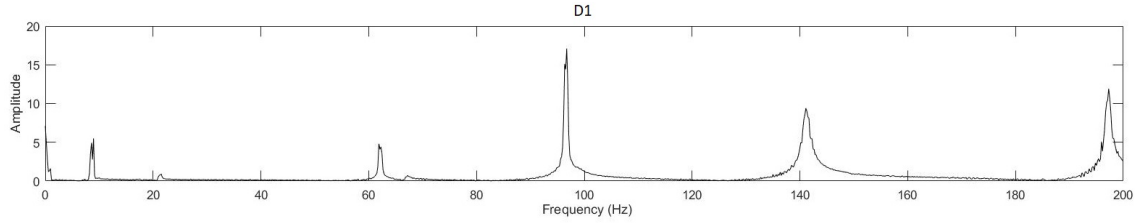

Figure E.9: Frequency response for position D1 on the Candide 3.0 ski.

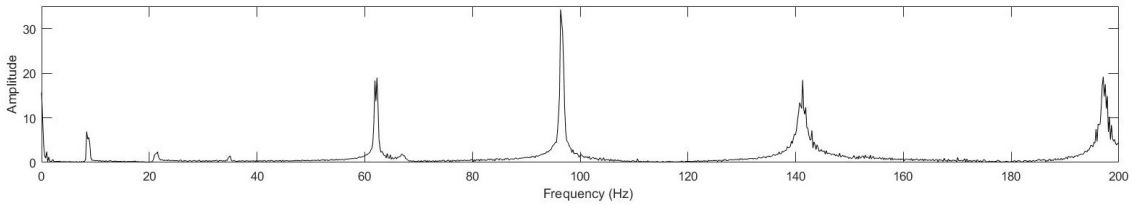

Figure E.10: Frequency response for position D2 on the Candide 3.0 ski.

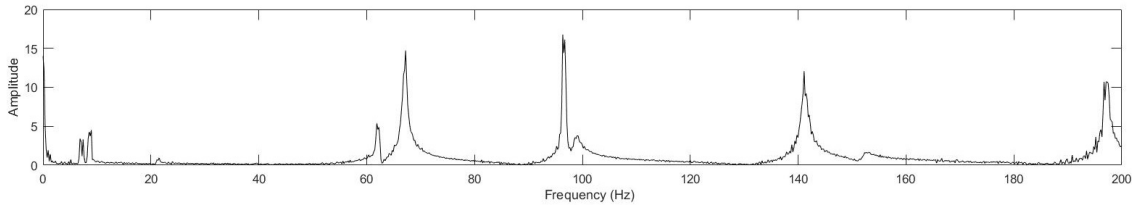

Figure E.11: Frequency response for position E1 on the Candide 3.0 ski.

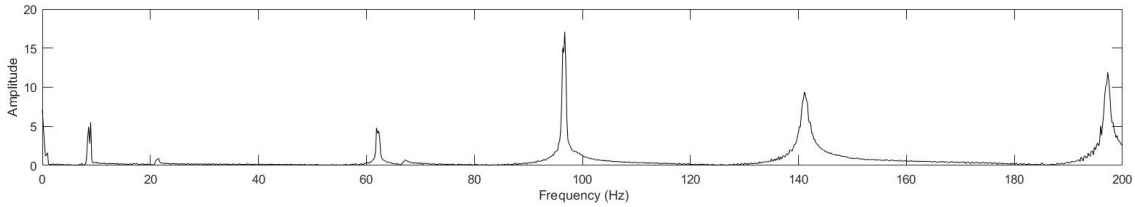

Figure E.12: Frequency response for position E2 on the Candide 3.0 ski.

F

Code for simple vibration test

```
#include <stdio.h>
#include <stdlib.h>
#include <string.h>
#include <ctype.h>
#include <avr/pgmspace.h>

const int trigPin = 9;
const int echoPin = 10;
long duration;

long startTime;
long elapsedTime;
long totalTime;

void setup() {
  // put your setup code here, to run once:
  pinMode(trigPin, OUTPUT);
  pinMode(echoPin, INPUT);
  Serial.begin(115200);
}

void loop() {
  startTime = micros();
  // put your main code here, to run repeatedly:
  digitalWrite(trigPin, LOW);
  delayMicroseconds(2);
  digitalWrite(trigPin, HIGH);
  delayMicroseconds(10);
  digitalWrite(trigPin, LOW);
  duration = pulseIn(echoPin, HIGH);
  Serial.println(duration);
  elapsedTime = micros() - startTime;
  delayMicroseconds(10000-elapsedTime);
  totalTime = micros() - startTime;
  //Serial.println(totalTime);
}
```

Figure F.1: The Arduino code for the simple vibration test.

The MATLAB code for the simple test

```
s = serial('COM4');
set(s,'BaudRate',115200);
fopen(s);
N = 2^9;
dT = 0.01;
T=(N-1)*dT;
t = 0:dT:T;
data = zeros(1,length(t));
flushinput(s);
for i=1:length(t)
    data(i) = str2num(fgetl(s));
end

subplot(1,2,1)
plot(t,data/58)
% Division by 58 to convert to cm from micro seconds traveltime
title('Motion')

subplot(1,2,2)
frekvenser=(([0:N])/(N*dT));
amplituder=abs(fft(data))/N;
amplituder(1)=1;
plot(frekvenser(1:length(frekvenser)/2),...
    amplituder(1:length(amplituder)/2))
title('Frequencies')

fclose(s)
delete(s)
clear s
```

G

Drawings

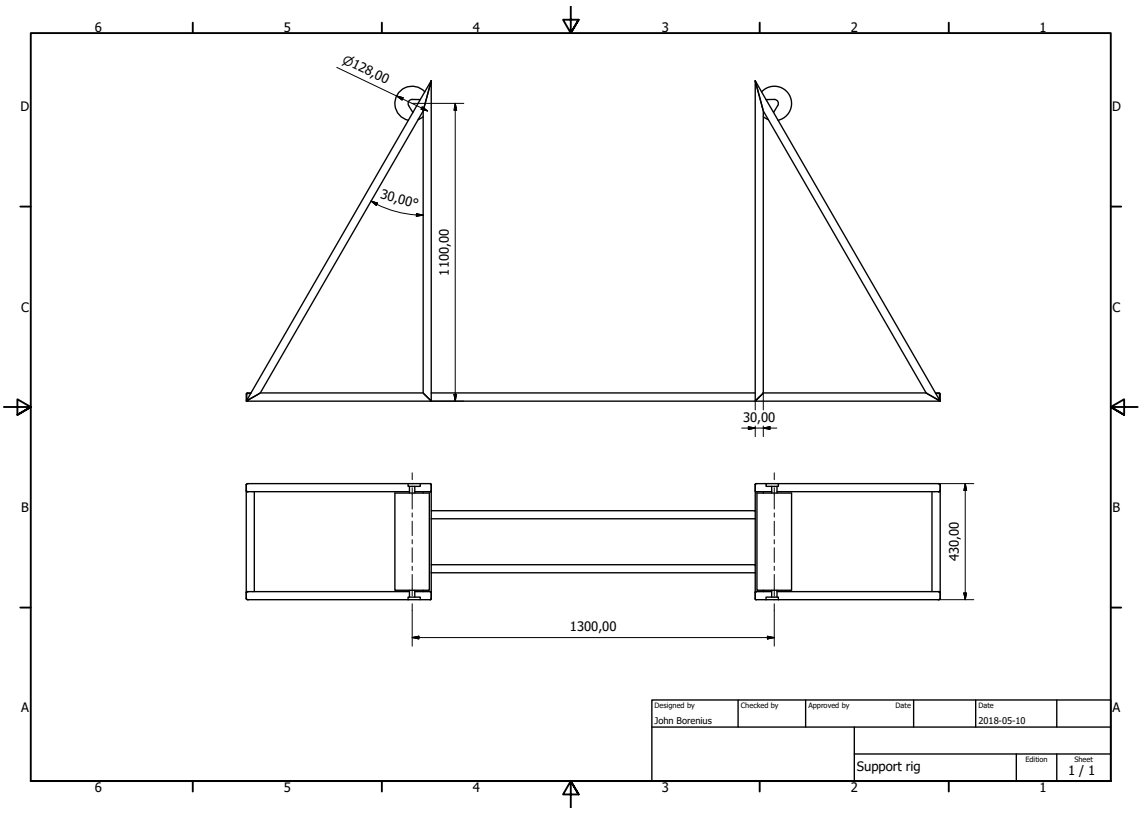

Figure G.1: Drawing of the test rig supports with only the vital dimensions.

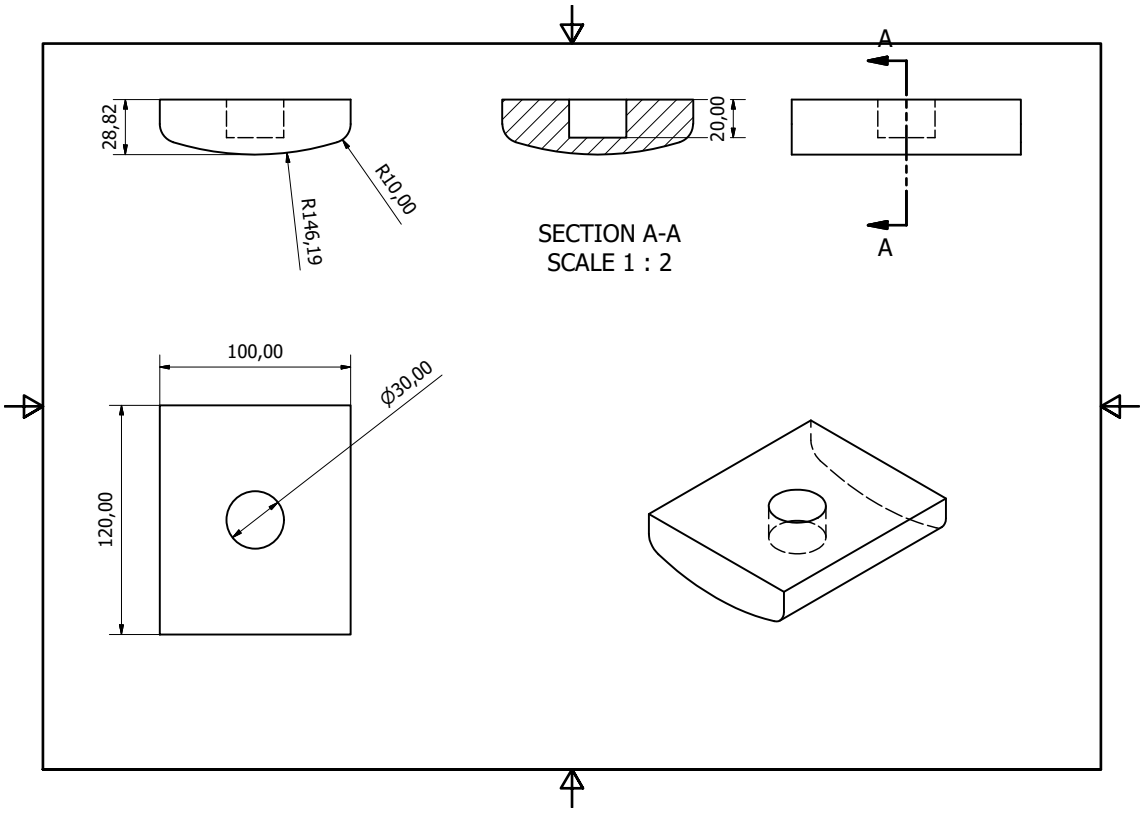

Figure G.2: Drawing of the tool which connects to the uniaxial compression test machine.

H

Material database

Name:	Type	Young's modulus x-driection	Poisson's ratio XY	Density
Steel	Metal	209GPa	0,27	8050 kg/m3
Titanal	Metal	72GPa	0,35	2820 kg/m3
Popplar	Wood	10,9 GPa	0,35	455 kg/m3
Balsa	Wood	3,71GPa	0,35	150 kg/m3
Ash	Wood	12,31GPa	0,35	680 kg/m3
Beech	Wood	14,31 GPa	0,35	720 kg/m3
Flax	Fiber reinforcement	27,6-100 GPa	0,25	
Paulownia	Wood	4,38 GPa	0,35	280 kg/m3
Carbon fiber UD	Fiber reinforcement	209 GPa	0,27	1540 kg/m3
ABS	Polymer	2,5 GPa	0,41	1020 kg/m3
Base (PE-UHMW)	Polymer	0,9 GPa	0,42	940 kg/m3
Glass fiber 1 (weak)	Fiber reinforcement	25 GPa	0,30	1989 kg/m3
Glass fiber 1 (stiff)	Fiber reinforcement	35 GPa	0,30	
Glass fiber 2 (weak)	Fiber reinforcement	20 GPa	0,30	2016 kg/m3
Glass fiber 2 (stiff)	Fiber reinforcement	35 GPa	0,30	

Figure H.1: Table of revised material database.